Applied Energy 239 (2019) 356–372

Contents lists available at ScienceDirect

Applied Energy

journal homepage: www.elsevier.com/locate/apenergy

Multi-objective optimization of energy arbitrage in community energy storage systems using different battery technologies

Tom Terlouw[a,b,1], Tarek AlSkaif[a,*,1], Christian Bauer[b], Wilfried van Sark[a]

[a] Copernicus Institute of Sustainable Development, Utrecht University, Princetonlaan 8a, 3584 CB Utrecht, the Netherlands
[b] Paul Scherrer Institute, Laboratory for Energy Systems Analysis, 5232 Villigen PSI, Switzerland

HIGHLIGHTS

- Multi-objective optimization of energy arbitrage in community energy storage systems.
- Economic feasibility from the perspective of an aggregator and a distribution system operator.
- Pareto frontiers of the two objectives for each scenario and six different battery technologies.
- Lithium-ion battery technologies show the best economic and environmental performance.
- The combination of energy arbitrage with peak shaving shows promising potential.

ARTICLE INFO

Keywords:
Community energy storage
Energy arbitrage
Peak shaving
Multi-objective optimization
Battery technologies

ABSTRACT

The power system requires an additional amount of flexibility to process the large-scale integration of renewable energy sources. Community Energy Storage (CES) is one of the solutions to offer flexibility. In this paper two scenarios of CES ownership are proposed. Firstly, an Energy Arbitrage (EA) scenario is studied where an aggregator aims to minimize costs and CO_2-emissions of an energy portfolio. Secondly, an Energy Arbitrage - Peak Shaving (EA-PS) scenario is assessed, which is based on a shared ownership between a Distribution System Operator (DSO) and an aggregator. A multi-objective Mixed Integer Linear Programming (MILP) optimization model is developed to minimize the operation costs and CO_2-emissions of a community situated in Cernier (Switzerland), using different battery technologies in the CES system. The results demonstrate a profitable system design for all Lithium-ion-Batteries (LiBs) and the Vanadium Redox Flow Battery (VRFB), for both the EA and EA-PS scenarios. The economic and environmental performance of the EA-PS scenario is slightly worse compared to the EA scenario, due to power boundaries on grid absorption and injection to achieve peak shaving. Overall, the differences between the EA and EA-PS scenarios, in economic and environmental performance, are small. Therefore, the EA-PS is recommended to prevent problematic loads on the distribution transformer. In addition, the Pareto frontiers demonstrate that LiBs perform best on both economic and environmental performance, with the best economic and environmental performance for the Lithium-Nickel-Manganese-Cobalt (NMC-C) battery.

1. Introduction

The power system is facing a tremendous change due to the large-scale integration of renewable Distributed Energy Resources (DERs) and the widespread of digitalization [1]. The International Energy Agency (IEA) expects that the share of renewables in the global electricity mix will increase to 30% in 2022, with a dominant share of wind and Photovoltaic (PV) power (82%) [2]. However, electricity generation from wind and solar is intermittent, and the current power system is not designed for such power variations [3]. Moreover, it is expected that the electrification of energy systems will increase even further, which inevitably results in larger power flows and ramps [4]. Therefore, the power system requires an additional amount of flexibility to ensure a resilient and reliable power system [5].

* Corresponding author.
E-mail addresses: t.m.terlouw@students.uu.nl (T. Terlouw), t.a.alskaif@uu.nl (T. AlSkaif), christian.bauer@psi.ch (C. Bauer), w.g.j.h.m.vansark@uu.nl (W. van Sark).
[1] These two authors contributed equally.

https://doi.org/10.1016/j.apenergy.2019.01.227
Received 2 October 2018; Received in revised form 14 January 2019; Accepted 27 January 2019

Nomenclature

Indices

a	index for shiftable loads, $a \in \{1, 2, ..., A\}$
t	index for time-slots, $t \in \{1, 2, ..., T\}$
i	index for households

Sets

$\mathscr{A}$	set of shiftable loads
$\mathscr{T}$	set of time-slots
$\mathscr{N}$	set of households in the community

Abbreviations

AIC	Akaike Information Criterion
ASHP	Air-to-water Source Heat Pump
BEV	Battery Electric Vehicle
BoS	Balance of System
CES	Community Energy Storage
DER	Distributed Energy Resource
DSM	Demand Side Management
DSO	Distribution System Operator
EA	Energy Arbitrage
EA-PS	Energy Arbitrage - Peak Shaving
EMS	Energy Management System
ESS	Energy Storage System
FiT	Feed-in-Tariff
HES	Home Energy Storage
IEA	International Energy Agency
LCA	Life Cycle Assessment
LCOE	Levelized Costs Of Electricity
LFP-C	Lithium–Iron-Phosphate/graphite
LiB	Lithium-ion Battery
MILP	Mixed Integer Linear Programming
NCA-C	Lithium-Nickel–Cobalt-Aluminium/graphite
NCA-LTO	Lithium-Nickel–Cobalt-Aluminium/ Lithium-Titanate-Oxide
NMC-C	Lithium-Nickel-Manganese-Cobalt-Oxide/graphite
O&M	Operation & Maintenance
PBP	Pay-Back-Period
PV	Photovoltaic
PVSC	PV-Self-Consumption
RE	Roundtrip Efficiency
SARIMA	Seasonal Auto Regressive Integrated Moving Average
SoC	State-of-Charge
STEM	Swiss Times Energy system Model
ToU	Time-of-Use
TSO	Transmission System Operator
VRFB	Vanadium Redox Flow Battery
VRLA	Valve Regulated Lead Acid

Parameters

η_{ch}	battery charging efficiency [–]
η_{dis}	battery discharging efficiency [–]
$C_{bat,average}$	average battery capacity during battery lifetime [kWh]
$C_{bat,CES}$	installed battery capacity of CES [kWh]
$C_{bat,req}$	required storage capacity for battery application [kWh]
DoD	depth of discharge [%]
w_1	weighting of costs [–]
w_2	weighting of CO_2-emissions [–]
E^a_{sl}	daily electricity consumption of a [kW]
EoL	share of battery capacity needed at the end of battery lifetime [–]
E_{tp}	energy throughput in the battery during battery lifetime [kWh]
N	number of households [–]
N_{cycles}	number of battery cycles during cycle lifetime [–]
$P_{bat,max}$	maximum power the battery can (dis)-charge [kW]
$P_{grid,max}$	maximum allowed aggregated power from/to the grid [kW]
P^t_{long}	long imbalance power at t [kW]
P^a_{max}	upper limit of power assignment to a [kW]
P^a_{min}	lower limit of power assignment to a [kW]
P^t_{nsl}	actual aggregated non-shiftable load at t [kW]
$\hat{P}^t_{nsl}$	predicted aggregated non-shiftable load at t [kW]
P^t_{PV}	actual power harvested by all PV systems at t [kW]
$\hat{P}^t_{PV}$	predicted power harvested by all PV systems at t [kW]
P_{trans}	capacity of the transformer [kW]
S	safety factor [kW]
SoC_0	initial battery SoC [%]
SoC_{max}	maximum battery SoC [%]
SoC_{min}	minimum battery SoC [%]
$TP^{a,t,i}$	time preference of i for the activation of a at t [–]

Variables

$p^{a,t,i}$	power demand of a in i at t [kW]
p^t	power action at t [kW]
$p^t_{bat,ch}$	battery charging power at t [kW]
$p^t_{bat,dis}$	battery discharging power at t [kW]
$p^t_{grid,absI}$	aggregated residual power absorbed from the grid in phase I at t [kW]
$p^t_{grid,absII}$	aggregated residual power absorbed from the grid in phase II at t [kW]
$p^t_{grid,inj}$	aggregated surplus power injected into the grid at t [kW]
p^t_{short}	imbalance power when aggregator is short at t [kW]
$p^{t,i}_{sl}$	aggregated shiftable loads of i at t [kW]
p^t_{sl}	aggregated shiftable loads in the community at t [kW]
$y^{a,t,i}$	binary decision variable when a can be operated in i at t [–]
SoC^t	battery state of charge at t [%]

Indicators

γ	discount rate [%]
B_{annual}	total annual benefits [euro/year]
c^t	actual intra-day electricity price at t [euro/kWh]
$\hat{c}^t$	predicted intra-day electricity price at t [euro/kWh]
C_{annual}	total annual costs [euro/year]
c_{annual}	annual costs for imbalance and electricity absorption [euro/year]
c^t_{hh}	household electricity price at t [euro/kWh]
$c_{maintenance}$	annual maintenance costs [euro/year]
$c^t_{paid,PV}$	remuneration paid to households for PV generation at t [euro/kWh]
$C_{imbalance}$	annual imbalance costs [euro/year]
c^t_{long}	imbalance price received when aggregator is long at t [euro/kWh]
c^t_{short}	imbalance price paid when aggregator is short at t [euro/kWh]
g^t	carbon intensity of grid power absorbed at t [kg CO_2-eq./kWh]
I_{CES}	investment costs in CES [euro]
I_{share}	share of potential annual incidents of total grid interactions [-]
L	lifetime of the system [years]
LCOE	levelized costs of electricity [euro/kWh]

LT_{bat}	lifetime of the battery pack [years]		[years]
LT_{cal}	calendric lifetime of the battery pack [years]	PVSC	Photovoltaic self-consumption ratio [–]
LT_{cyc}	cycle lifetime of the battery pack [years]	R_{annual}	total annual revenue [euro/year]
PBP	number of years before the investment is recovered		

One solution to achieve a more flexible power system is to implement smart technologies, such as Energy Management Systems (EMSs) [6]. EMSs can be useful to enhance the implementation of other key solutions, such as Demand Side Management (DSM) and Energy Storage Systems (ESSs). DSM and ESSs can improve the flexibility of the power system by offering additional applications to Transmission System Operators (TSOs) and Distribution System Operators (DSOs), such as the provision of ancillary services and peak shaving [7]. In addition, applications can be combined in order to increase the profitability of an ESS [8].

Current developments demonstrate that an aggregator can provide trading in electricity markets due to the aggregation of Home Energy Storage (HES) systems [9]. An aggregator can be defined as "a company who acts as an intermediary between electricity end-users, DER owners and power system participants who wish to serve these end-users or exploit the services provided by these DERs" [10]. In this way, the aggregator can provide flexibility and energy trading more easily [9,11].

On the other hand, there is an increasing interest in Community Energy Storage (CES) systems, due to beneficial economies of scale and optimal storage sizes in CES compared to HES [8,12–14]. CES can be defined as an "ESS located at the consumption level which can perform several applications with a positive impact for both end users and the network" [15]. It is expected that CES will offer distributed applications and energy trading in electricity markets more efficiently, since the controlling of CES is expected to be more convenient than the controlling of HES [8]. For example, a CES system requires only one communication system and EMS, while these are required for each household in a HES system. Consequently, different studies aim to capture additional benefits of CES, when providing a combination of applications.

For example, the potential benefits from multiple CES deployment in a distribution system were assessed in [16]. The work in [17] concluded that the economic benefits from stationary battery systems can be improved by combining battery applications. In [18], a model was proposed to determine the benefits of stationary battery storage for a DSO and an aggregator, and the competition of ownership between these stakeholders was compared. The work in [19] suggested an optimal bidding strategy for a battery owned by an aggregator in the Spanish day-ahead and intra-day electricity market. An approach to facilitate a DSO to optimally design the CES system, while considering transformer aging and the voltage profile of the system, was proposed in [20]. In [21], a multi-objective optimization framework of an ESS was developed to optimize the daily operation of a smart grid with a high penetration of sensitive loads. In [22], a strategy was proposed to maximize the revenue obtained from CES systems in a competitive electricity market. The work in [23] proposed a strategy for the optimal operation of distribution networks in the presence of DERs and battery ESSs.

However, a techno-economic assessment of CES systems for Energy Arbitrage (EA) in the intra-day market, which includes both environmental and economic impacts in the perspective of different CES owners and using different battery technologies, is largely missing. Furthermore, there is a lack of case studies which determine the impact on the transformer in the distribution network when residential energy systems shift towards all-electric energy systems. To increase comparability, we introduce an initial scenario where heat is supplied by natural gas and electricity is only used for electrical appliances.

We focus on EA since this is one of the most profitable applications CES systems could offer in the near future when CES applications are combined [17]. However, the implementation of EA could result in large power flows and problems related to the transformer distribution capacity [18]. Therefore, we include peak shaving as an additional application from the DSO perspective. Our work aims to determine the annual costs, CO_2-emissions and profitability of EA and peak shaving in a case study in the perspective of different CES owners, based on different battery technologies.

The battery technology portfolio considered in this research includes four Lithium-ion-Batteries (LiBs): Lithium-Iron-Phosphate/graphite (LFP-C), Lithium-Nickel-Cobalt-Aluminium-Oxide/graphite (NCA-C), NCA/Lithium-Titanate-Oxide (NCA-LTO) and Lithium-Nickel-Manganese-Cobalt-Oxide/graphite (NMC-C). LiBs batteries represent the most promising current and near-future alternatives for decentralized electricity storage [24–26]. Besides LiBs, the Valve Regulated Lead Acid (VRLA) battery and the Vanadium Redox Flow Battery (VRFB) are included since these batteries are widely used in stationary battery applications [27,28]. In addition, a detailed performance and cost data as well as life cycle inventories are available for the selected battery portfolio [29].

The contribution of this paper can be summarized as follows:

- A multi-objective optimization framework for energy arbitrage using a CES system considering two ownership scenarios.
- A comprehensive feasibility analysis and techno-economic and environmental assessment of the CES system from the perspective of an aggregator and a DSO.
- A detailed performance analysis of six different battery technologies in the CES system considering their technical, economic and environmental parameters.
- Applying the proposed optimization and assessment framework on a realistic case study of all-electric residential energy systems in Switzerland.

The rest of the paper is organized in the following way: Section 2 explains the system description of the CES system. Next, the optimization problem is formulated in Section 3. Data collection is presented in Section 4. Performance indicators are discussed in Section 5. After that, the results are presented in Section 6. Finally, the discussion and conclusion are given in Sections 7 and 8, respectively.

2. System design

In this work, a residential energy system is considered which consists of a number of households (N), which have an electricity and heat demand profile. We focus on all-electric energy systems since we expect that residential energy systems will shift towards all-electric energy systems due to more aggressive climate policy [30].

We aggregate the individual heat and electricity demand loads as well as PV generation of a set of households in a community $\mathcal{N}$, indexed by $i \in \{1, 2, ..., N\}$, which results in an aggregated heat and electricity demand and PV generation profiles. The aggregated demand and PV supply can be delivered during a number of timeslots, $t \in \mathcal{T} = \{t_0, t_0 + \Delta t, t_0 + 2\Delta t, ..., T\}$. The considered number of timeslots for a time horizon is represented by T. In addition, each household contains a set of shiftable loads $\mathcal{A}$, indexed by $a \in \{1, 2, ..., A\}$, and non-shiftable load. Shiftable loads (P^t_{sl}, e.g. Battery Electric Vehicles (BEVs)) can be scheduled at preferred timeslots and can offer flexibility in DSM strategies. While non-shiftable loads (P^t_{nsl}, e.g. TV) are bound to

a fixed operational period and cannot be used for DSM strategies. We include a high penetration of shiftable load in the form of BEVs, since the share of passenger BEVs is expected to increase significantly in the coming decades [31]. For simplicity, it is assumed that the heat supply in the all-electric scenario is non-shiftable since this reduces the system design and computation time significantly. An Air-to-water Source Heat Pump (ASHP) model is adopted from [32] to determine the power demand for space heating and domestic hot water.

Fig. 1 presents the system description of the CES system. We assume that the CES battery is owned by a DSO and/or an aggregator (see Sections 3.1 and 3.2). Furthermore, we include a high penetration level of renewable electricity by assuming that each household owns a PV system. The aggregated electricity and electric heat demand of the community can be satisfied by absorption of electricity from the grid, by direct consumption of rooftop PV or by discharging the CES battery ($p^t_{bat,dis}$). The localized generation of PV-electricity (P^t_{PV}) can be directly consumed, can be stored in the CES battery by charging the battery ($p^t_{bat,ch}$), or can be injected into the electricity grid ($p^t_{grid,inj}$).

In addition, each household owns a localized EMS to schedule and control the shiftable and non-shiftable loads. The localized EMSs communicate with the community EMS to optimize the scheduling and the load of the community. The capacity of the transformer (P_{trans}) is included to examine the impact of the community on the transformer in the distribution network. Next, the battery size is determined.

Firstly, the battery is oversized to ensure the required storage capacity ($C_{bat,req}$) at the end of the battery lifetime. The installed energy size ($C_{bat,CES}$) of the CES battery technology is determined with Eq. (1), considering the depth-of-discharge (DoD), the discharge efficiency (η_{dis}) and the rated energy capacity the battery should operate on the end of its life (EoL) [29].

$$C_{bat,CES} = \frac{C_{bat,req}}{\eta_{dis} \cdot DoD \cdot EoL} \quad (1)$$

Next, we consider battery degradation in the optimization problem since the battery degrades per charging/discharging cycle (i.e. cycle losses) and by time (i.e. calendar losses) [29]. This can have a large effect on the economic profitability, as a reduced performance of the battery can reduce the economic feasibility of a system lay-out hence can increase costs [33]. Consequently, we include battery degradation in a simplified way by oversizing the batteries and by implementing a constraint to ensure the lifetime of the battery.

The battery lifetime can be limited by the cycle lifetime (i.e. cycle losses) or the calendrical lifetime (i.e. calender losses). The cycle lifetime is the equivalent number of years the battery can operate according to operating conditions of a battery application. In this work, the primary battery application is EA, where we include a large amount of shiftable loads (i.e. in the form of BEVs) and a high penetration of community generated PV electricity. Therefore, we assume that the battery is extensively used and that there is one daily battery discharge. Hence, this leads to a minimum of 365 cycles per year for each battery technology. Furthermore, the battery is subjected to calendrical aging, which refers to the number of years when the battery pack does not fulfill its requirements in terms of energy required per discharging cycle [34]. The battery lifetime (LT_{bat}) is obtained from taking the minimum of the calendrical lifetime (LT_{cal}) and cycle lifetime (LT_{cycle}) of the battery technology.

We aim to avoid battery stresses hence battery pack replacements before the battery lifetime is reached. In addition, we aim to make the comparison as fair as possible to ensure that the battery lifetimes of the battery technologies are respected. The following steps are required for the inclusion of battery degradation in the optimization problem (see Eq. (19)). Firstly, the average battery capacity ($C_{bat,average}$) during the battery lifetime is determined, considering the required CES battery capacity at the end of the battery lifetime.

$$C_{bat,average} = \frac{(EoL + 1)}{2} \cdot C_{bat,CES}. \quad (2)$$

In addition, we assume that the state of health of the battery degrades linearly per lifetime year. Therefore, we use the average battery capacity ($C_{bat,average}$) of each battery technology in the optimization problem to increase the comparability between battery technologies. In reality, battery degradation is more complicated and depends heavily on different stress factors, such as the C-rate, DoD and temperature which usually results in a non-linear relationship (e.g. see [35]). However, detailed battery degradation modelling is out of the scope of this research.

The energy throughput of the battery is calculated to determine the amount of energy the battery can process (E_{tp}) during the battery lifetime.

$$E_{tp} = \eta_{dis} \cdot N_{cycles} \cdot C_{bat,average} \cdot \frac{DoD}{100}. \quad (3)$$

Next, the multi-objective optimization problem is formulated to determine the optimal system operation of the residential energy system with different scenarios of CES ownership, considering both costs and CO_2-emissions.

3. Multi-objective optimization problem

In this work, the main objective is to minimize annual operation costs from grid electricity absorption and grid CO_2-emissions. Electricity consumption of households can be shifted to periods when grid electricity prices (c^t) are low (i.e. DSM). Besides costs, the reduction of CO_2-emissions is getting more importance in the built environment [36,37]. Therefore, a second objective is added to minimize CO_2-emissions during system operation.

A Mixed Integer Linear Programming (MILP) approach is used since MILP is a well-established and accurate optimization tool [38]. Gurobi (v 8.0) is implemented in Python (v 3.6) to develop the optimization under a set of constraints [39]. Next, two different scenarios of CES ownership are proposed and six battery technologies will be used in assessing the economic and environmental potential of the proposed system (i.e., see Table 1). The objectives and constraints of each scenario are explained in Sections 3.1 and 3.2. A monolithic flowchart of the proposed approach is presented in Fig. 2.

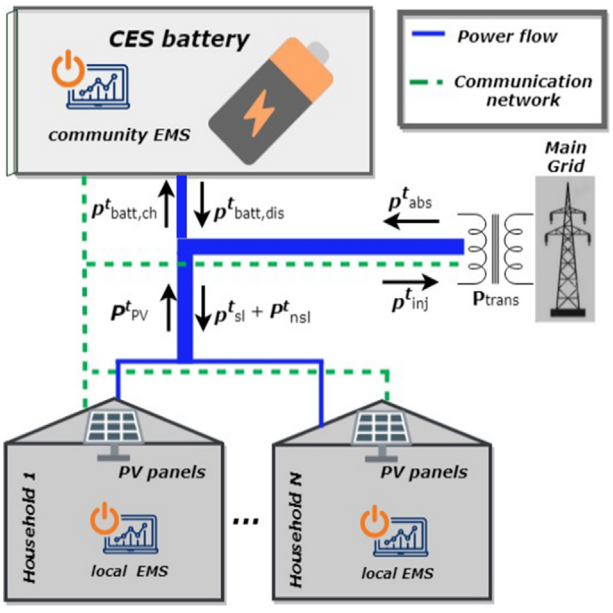

Fig. 1. System description in CES.

Table 1
Technology specific input parameters for a required CES battery size of 165 kWh ($C_{bat,req}$).

	NMC-C	LFP-C	NCA-C	NCA-LTO	VRLA	VRFB	Unit
$C_{bat,CES}$	235	238	235	216	433	254	kWh
$C_{bat,average}$	212	214	212	195	390	228	kWh
$P_{bat,max}$	82.5	82.5	82.5	82.5	82.5	82.5	kW
RE	89	87	89	91	75	66	%
DoD	93	93	93	100	55	100	%
N_{cycles}	4996	6529	2498	15,000	1500	13,000	Cycles
LT_{cycle}	13.7	17.9	6.84	41.1	4.11	35.6	Years
LT_{cal}	12	12	12	23	9	19	Years
LT_{bat}	12	12	6.84	23	4.11	20[a]	Years
Battery packs needed	1.00	1.00	1.75	0.52	2.92	0.60	–
BoS lifetime	20	20	20	20	20	20	Years
EoL	80	80	80	80	80	80	%
Costs							
Pack cost	335	461	281	900	263	428	euro/kWh
BoS cost	316	316	316	316	316	1064	euro/kW
O&M cost	9	9	9	9	9	43	euro/kW/year
CO_2-emissions production							
Pack	108.3	117.9	125.6	373.4	74.1	142.9	kg CO_2-eq./kWh
BMS & EMS	26.6	26.6	26.6	26.6	26.6	N.A.	kg CO_2-eq./kWh
Power unit	28.2	28.2	28.2	28.2	28.2	259.5	kg CO_2-eq./kW

[a] VRFB is assumed to have the same lifetime as the BoS lifetime [34].

3.1. Energy arbitrage scenario

The EA scenario is based on an aggregator which trades in the electricity market. In Europe, trading in the day-ahead and intra-day market has grown significantly in the past decennia [40]. In the day-ahead market, electricity is traded on a daily basis and energy traders must submit their electricity bid a day before delivery time. While in the intra-day market, electricity is traded on the same day and the bid can be submitted an hour before delivery time.

In both cases, it is essential to predict the consumption or generation adequately to decrease prediction errors hence penalties from deviation of the electricity bid. The following assumptions are made in the problem design. Firstly, it is assumed that the battery is owned by an aggregator and/or DSO. Secondly, no additional grid tariffs (e.g. fixed tariffs) are implemented by the TSO and it is assumed that all bids of the aggregator are accepted. Furthermore, the sell and buy prices in the intra-day market are assumed to be the same. Also, it is expected that prices on the electricity market are not influenced by the bids of the aggregator, since we assume that the aggregator is considerably small compared to the intra-day electricity market.

In the EA scenario, an aggregator is introduced as a CES owner. This aggregator acts as a buyer of electricity in the intra-day-market. The main goal of the aggregator in this study is to manage the energy portfolio of the community in a most cost-efficient and environmental friendly way by minimizing electricity costs and CO_2-emissions [19]. However, with the increased penetration of intermittent renewable energy the prediction becomes more complicated [40]. Consequently, we assess the intra-day market, since the prediction error and complexity of the bidding scheme reduce significantly compared to the day-ahead market [19].

The EA scenario consists of two phases: phase I and phase II. The purpose of phase I is to optimize the bid by minimizing grid absorption in the intra-day market one-hour before delivery time. While in phase II, the actual loads, PV generation and electricity prices are determined in order to minimize possible imbalance costs derived from the submitted bid from phase I. These phases are illustrated in Fig. 3 and described in more detail in Sections 3.1.1 and 3.1.2.

3.1.1. Phase I: Bidding

We consider two costs in the system: grid absorption costs during phase I and imbalance costs during phase II (see Figs. 2 and 3). In phase I, the first multi-objective optimization is formulated. The purpose of phase I is to optimize the scheduling of the community load based on the predicted aggregated demand, PV generation and electricity prices in order to reduce penalties from deviation of the submitted bid. We assume that the aggregator acts as a buyer in the electricity market since the PV generation from households is considerably small to act as a seller. Therefore, at each timeslot $t-1$, an aggregator can decide to buy or to take no action. Note that the aggregator predicts future electricity prices to schedule loads in a most cost-efficient way by making use of DSM strategies. The model used to predict loads, PV generation and electricity prices is explained in Section 4.4. In the optimization model, the predicted values are made available for each timeslot and each day of the assessment period. This means that the vectors of predicted values serve as inputs to the optimization problem in phase I. This enables to calculate the imbalance costs in phase II (see Section 3.1.2) in order to assess their impact on the economic and environmental performance of the CES system for an aggregator.

Next, the multi-objective function is determined for phase I (see Eq. (4)) in order to develop the bid at $t-1$, based on predicted aggregated PV generation ($\widehat{P}^t_{PV}$), predicted aggregated non-shiftable community load ($\widehat{P}^t_{nsl}$) and predicted intra-day electricity prices ($\widehat{c}^t$). Since the aggregator aims to maximize profits, it follows that costs of electricity absorbed from the grid must be minimized to obtain the electricity portfolio of the community in the most cost-effective way. In addition, the second objective is the minimization of CO_2-emissions from the grid (g^t) during system operation. It is expected that CO_2-emission prices will increase [41] and environmental regulations will become more strict in the coming decades to achieve climate goals [4]. Therefore, the minimization of CO_2-emissions is considered as important from the perspective of the aggregator.

$$\begin{aligned} &\text{minimize} \quad \{w_1 f_1\left(P^t_{grid,absI}\right), w_2 f_2\left(P^t_{grid,absI}\right)\}, \\ &\text{where:} \quad f_1 = \sum_{t=1}^{T} \widehat{c}^t p^t_{grid,absI} \Delta t, \\ &\qquad\qquad f_2 = \sum_{t=1}^{T} g^t p^t_{grid,absI} \Delta t, \end{aligned} \tag{4}$$

where w_1 is the weighting of costs [–], w_2 is the weighting of

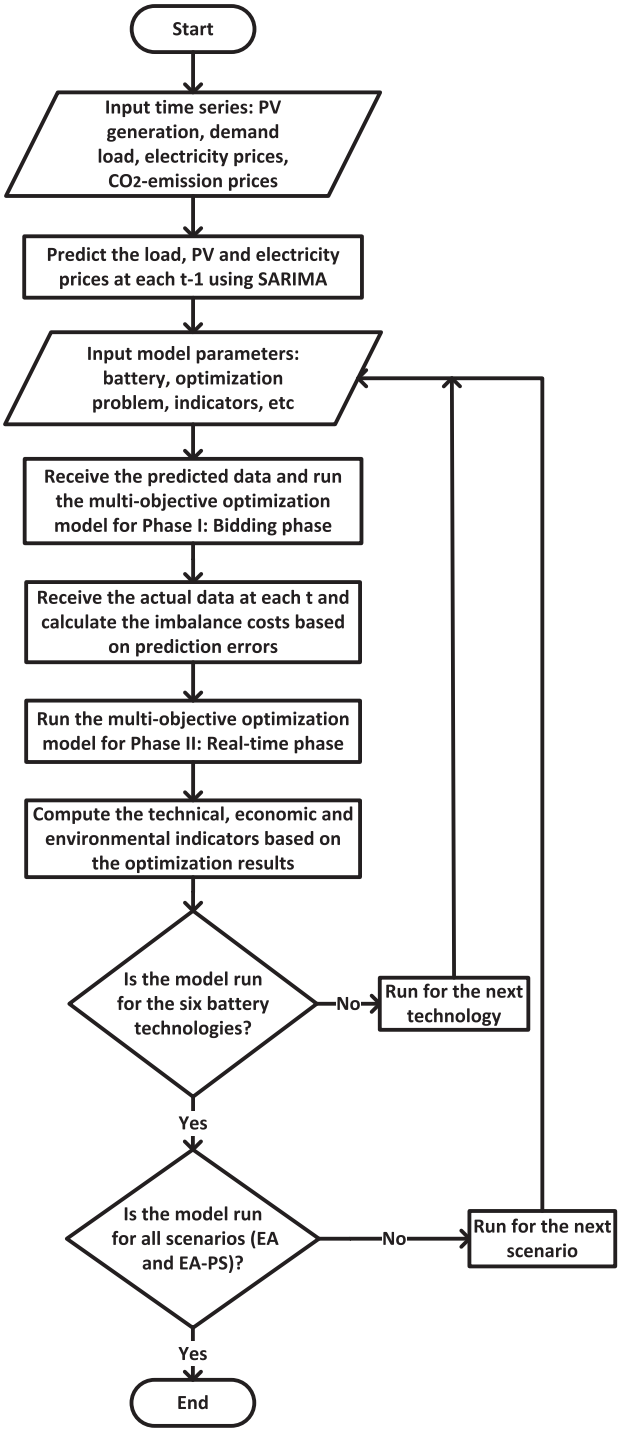

Fig. 2. Flowchart of the proposed approach.

CO_2-emissions [–], $p^t_{\text{grid,absI}}$ is the aggregated residual power absorbed from the grid in phase I at t [kW] and Δt represents the timestep.

Different constraints are active to let the community system operate in a smooth way. The following model is adopted from [14].

3.1.1.1. Total balance of system. A system balance is implemented to meet the supply and demand of the community. At each timeslot, a power action (p^t) can be expected. This power action can be an interaction with the electricity grid (absorbing/injecting power), and/or an interaction with the CES battery (charging/discharging power).

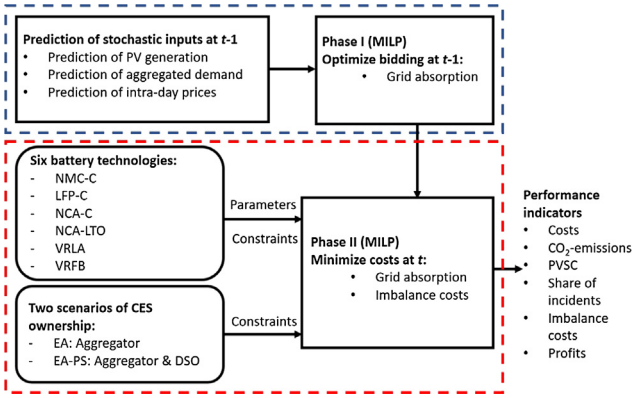

Fig. 3. The strategy of the aggregator in phase I and phase II.

$$p^t = \left(p^t_{\text{grid,absI}} - p^t_{\text{grid,inj}}\right) + \left(p^t_{\text{bat,dis}} - p^t_{\text{bat,ch}}\right), \quad \forall\, t. \tag{5}$$

In addition, the following constraint is implemented to ensure the balance between the aggregated supply and demand of the community.

$$p^t = p^t_{\text{sl}} + \hat{P}^t_{\text{nsl}} - \hat{P}^t_{\text{PV}}, \quad \forall\, t. \tag{6}$$

3.1.1.2. Power boundaries of main grid and CES battery. The maximum absorbed or injected power from or to the electricity grid is set equal to the maximum allowed aggregated power from or to the grid ($P_{\text{grid,max}}$). In this way, the capacity of the transformer is not considered. This choice is made since the aggregator in this scenario (i.e., EA) aims to minimize costs and CO_2-emissions while neglecting power boundaries of the transformer in the distribution network. This seems reasonable as system operators are still obliged to connect decentralized energy systems.

$$0 \leqslant p^t_{\text{grid,absI}} \leqslant P_{\text{grid,max}}, \quad \forall\, t, \tag{7}$$

$$0 \leqslant p^t_{\text{grid,inj}} \leqslant P_{\text{grid,max}}, \quad \forall\, t. \tag{8}$$

Furthermore, power boundaries are active to avoid imbalances in the CES battery. The charging and discharging power should not exceed the maximum CES battery charging and discharging power.

$$0 \leqslant p^t_{\text{bat,ch}} \leqslant P_{\text{bat,max}}, \quad \forall\, t, \tag{9}$$

$$0 \leqslant p^t_{\text{bat,dis}} \leqslant P_{\text{bat,max}}, \quad \forall\, t. \tag{10}$$

3.1.1.3. Battery energy storage system. The dynamics of the CES battery can be described by its State of Charge (SoC) at each timeslot t.

$$\text{SoC}^t = \text{SoC}^{t-1} - \left(\frac{1}{\eta_{\text{dis}} C_{\text{bat,average}}}(p^t_{\text{bat,dis}})\Delta t - \frac{\eta_{\text{ch}}}{C_{\text{bat,average}}}(p^t_{\text{bat,ch}})\Delta t\right), \quad \forall\, t. \tag{11}$$

The SoC of the CES battery at each t must respect the minimum (SoC_{min}) and maximum SoC (SoC_{max}).

$$\text{SoC}_{\text{min}} \leqslant \text{SoC}^t \leqslant \text{SoC}_{\text{max}}, \quad \forall\, t. \tag{12}$$

Furthermore, we assume that the CES battery should have at least the same charging potential as the day before to ensure an equal daily charging potential.

$$\sum_{t=1}^{T} \text{SoC}^t - \text{SoC}^{t-1} \geqslant 0, \quad \forall\, t. \tag{13}$$

3.1.1.4. Shiftable load. The shiftable loads of households in the community provide flexibility and are optimally scheduled respecting

their individual operation constraints and time preference. For simplicity, the only shiftable loads considered in this work are BEVs. However, other shiftable loads can be easily incorporated into the model considering the constraints which are described below.

Households might have different set of shiftable loads. The total energy scheduled to each shiftable load a in household i per day should meet its daily required amount of energy (E^a_{sl}).

$$\sum_{t=1}^{\mathrm{T}} p^{a,t,i}\Delta t = E^a_{\mathrm{sl}}, \quad \forall\, a. \tag{14}$$

Furthermore, the shiftable power of a device should be in between the boundaries of its maximum ($P^a_{\max}$) and minimum charging power ($P^a_{\min}$).

$$y^{a,t,i}P^a_{\min} \leqslant p^{a,t,i} \leqslant y^{a,t,i}P^a_{\max}, \quad \forall\, a,\, t, \tag{15}$$

where $y^{a,t,i}$ is a binary decision variable that is activated when the shiftable load in i can be scheduled according to the time preference of i. The time preference ($\mathrm{TP}^{a,t,i}$) for scheduling the shiftable loads in i is respected with Eq. (16).

$$y^{a,t,i} \leqslant \mathrm{TP}^{a,t,i}, \quad \forall\, a,\, t. \tag{16}$$

The total power assigned to all shiftable loads in household i at t is equal to its total shiftable load demand at t.

$$\sum_{a=1}^{\mathrm{A}} p^{a,t,i} = p^{t,i}_{\mathrm{sl}}, \quad \forall\, t. \tag{17}$$

Consequently, the aggregated shiftable load of the whole community at t (i.e., used in Eq. (6)) is given by summing up the total shiftable load demand over all households T.

$$\sum_{i=1}^{\mathrm{N}} p^{t,i} = p^t_{\mathrm{sl}}, \quad \forall\, t. \tag{18}$$

3.1.1.5. Battery degradation. Battery degradation is included in a simplified way by setting a constraint on battery utilization (see Section 2). The following constraint is active to ensure that the battery lifetime ($\mathrm{LT_{bat}}$) is respected, which is the minimum of the calendric lifetime ($\mathrm{LT_{cal}}$) and cycle lifetime ($\mathrm{LT_{cycle}}$). This way, the maximum number of cycles (cycle lifetime) and the calendric lifetime of the battery are considered in the system operation. Note that our optimization covers one year ($t = 8760$ h). Therefore, the energy throughput ($\mathrm{E_{tp}}$) was calculated based on the average CES capacity (see Eqs. (2) and (3)).

$$\mathrm{LT_{bat}} \sum_{t=1}^{8760} p^t_{\mathrm{bat,dis}} \leqslant \mathrm{E_{tp}}, \quad \forall\, t. \tag{19}$$

Now that the optimization problem is formulated at t-1, the aggregator can optimize grid interaction based on the predicted loads, PV generation and electricity prices to submit the electricity bid at t-1. In the next section, the actual loads and electricity prices will be used for the optimization in phase II at timeslot t.

3.1.2. Phase II: Real time

After the bidding scheme is submitted, actual demand loads (P^t_{nsl}), PV generation (P^t_{PV}) and electricity prices (c^t) are identified at timeslot t to replace the predicted demand ($\widehat{P}^t_{\mathrm{nsl}}$), predicted PV generation ($\widehat{P}^t_{\mathrm{PV}}$) and predicted electricity price ($\hat{c}^t$), respectively. Therefore, phase II of the optimization starts. At certain moments, it can be expected that imbalance costs should be paid due to prediction errors derived from the bid in phase I. Hence, a second term is added which covers imbalance costs for the aggregator (see Eq. (21)).

The imbalance power is obtained from taking the difference of grid absorption between the submitted bid (in phase I) and the actual consumption of the aggregator (in phase II). Note that only positive differences are taken into account (see Eq. (20)). An imbalance cost has to be paid when the real absorption of electricity ($p^t_{\mathrm{grid,absII}}$) in phase II is higher than the expected absorption of the submitted bid ($p^t_{\mathrm{grid,absI}}$) in phase I.

$$p^t_{\mathrm{short}} = \begin{cases} p^t_{\mathrm{grid,absII}} - p^t_{\mathrm{grid,absI}} > 0 & : p^t_{\mathrm{grid,absII}} - p^t_{\mathrm{grid,absI}}, \\ p^t_{\mathrm{grid,absII}} - p^t_{\mathrm{grid,absI}} \leqslant 0 & : 0. \end{cases} \tag{20}$$

This means that the aggregator has a deficit of power and is "short" (p^t_{short}) hence the second term in Eq. (21) is activated. In this case, the "short" imbalance price has to be paid (c^t_{short}). In contrast, when the consumption is lower than submitted in the bid, the long price is received and the aggregator is "long'. Also, when more electricity is generated than expected, the aggregator can inject the surplus electricity into the grid (i.e. aggregator is "long") hence we assume that the aggregator receives the "long" price (c^t_{long}). Note that the long price may be negative. In this way, the aggregator does not receive remuneration but has to pay for grid injection.

We decide to not include remuneration for the injection of grid electricity in the multi-objective function. The end-user customer prices are usually higher than remuneration prices for grid injection, hence more profit can be made from delivering electricity to the end-user customer. Consequently, grid injection should be avoided. Ultimately, this leads to the following multi-objective function for the EA scenario. The optimization constraints of the real-time phase problem are the same constraints used in the bidding phase (i.e., Eqs. (5)–(19)). For the sake of avoiding repetition, those constraints are not rewritten in this section.

$$\begin{aligned} &\text{minimize} \quad \{w_1 f_1\left(p^t_{\mathrm{grid,absII}}\right),\, w_2 f_2\left(p^t_{\mathrm{grid,absII}}\right)\}, \\ &\text{where:} \quad f_1 = \sum_{\mathrm{t=1}}^{\mathrm{T}} \left(c^t p^t_{\mathrm{grid,absII}}\Delta t + c^t_{\mathrm{short}} p^t_{\mathrm{short}}\Delta t\right), \\ &\qquad\qquad f_2 = \sum_{\mathrm{t=1}}^{\mathrm{T}} g^t p^t_{\mathrm{grid,absII}}\Delta t. \end{aligned} \tag{21}$$

3.2. Energy Arbitrage - Peak Shaving scenario

The Energy Arbitrage - Peak Shaving (EA-PS) scenario is based on a shared ownership of the CES unit between an aggregator and a DSO. The objectives of the aggregator and the DSO might contradict. The aggregator aims to minimize annual costs and CO_2-emissions by minimizing imbalance costs and electricity absorption. While the DSO aims to achieve peak shaving in order to reduce system contingencies by reducing the load on the distribution transformer [18].

Consequently, all constraints of the EA scenario hold for this scenario except Eqs. (7) and (8) which are modified to achieve peak shaving. This modification ensures that the transformer capacity ($\mathrm{P_{trans}}$), predefined by the DSO, is respected. A safety factor (S) can be added to prevent that the transformer power is (too) close to the maximum transformer capacity.

$$0 \leqslant p^t_{\mathrm{grid,absI}} \leqslant \mathrm{P_{trans}} - \mathrm{S}, \quad \forall\, t, \tag{22}$$

$$0 \leqslant p^t_{\mathrm{grid,inj}} \leqslant \mathrm{P_{trans}} - \mathrm{S}, \quad \forall\, t. \tag{23}$$

The same strategy is implemented as explained in Section 3.1. All earlier described constraints are also applicable to this scenario, unless described otherwise in this section.

4. Data and model inputs

4.1. Households

Demand data is derived from the aggregated demand loads of a

community of 22 households situated in Cernier (Switzerland) for the year 2014–2015. Cernier is located in the North-West of Switzerland in the Swiss canton Neuchâtel at an altitude of 820 meters. For a more detailed analysis and data of this community, please refer to [13].

Furthermore, we implement different measures to encourage residential households to deliver their PV electricity to the CES battery. Firstly, households are paid by the CES owner. Residential households obtain this benefit in the form of a Feed-in-Tariff (FiT). In our case study, the CES owner remunerates residential households with the same FiT as paid by the Swiss government for larger PV systems (i.e. larger than 30 kW_p) in Switzerland, which is approximately 0.10 euro/kWh (i.e. 0.11 CHF/kWh [42,43]).

This offer is beneficial since FiTs are not applicable in Switzerland for end-user customers (for small PV systems between 2 and 10 kW_p [43,44]). Households only obtain a subsidy from the Swiss government on their PV investment, with a maximum of 30% of the initial PV investment. In our case study, households can both benefit from the subsidy and the FiT paid by the CES owner. Therefore, we assume that each household participate in the CES system. We select the FiT remuneration for the sensitivity analysis since we expect that the economic profitability of the CES owner is highly influenced by the FiT.

Furthermore, a beneficial Time-of-Use (ToU) pricing scheme is offered to charge the end-user customer for their electricity consumption. A ToU price scheme is implemented by most electricity suppliers in Switzerland [45]. In our case study, a price scheme is adopted from a local electricity supplier in Cernier. A high electricity price tariff is applied from 7.00 to 21.00, also during weekends. At these moments, the electricity price is defined at 0.183 euro/kWh. The low electricity price is specified on 0.101 euro/kWh and is active during night times (21.00–7.00) [46].

Moreover, we assume that each household owns a BEV and drives 37 km each day, which is the average daily distance travelled in Switzerland [47]. Smart charging is used to obtain the most beneficial electricity price and CO_2-emission timeslot for BEV charging. In addition, we assume that the BEV can be charged only during night times (21.00–7.00).

4.2. Hourly emission factors

Hourly CO_2-emissions from the grid are obtained from the Swiss Times Energy system Model (STEM)[2]. The STEM contains information about the hourly dispatch of electricity generation units in Switzerland [48]. The electricity generation includes both (renewable) electricity generation and import of electricity from neighbouring countries. The hourly market shares of different generation technologies (e.g. hydropower, coal-based, nuclear, natural-gas based, PV, geothermal and wind) are multiplied by CO_2-emission factor of each generation technology using a Life Cycle Assessment (LCA) approach specified for Switzerland [49]. These emission factors are based on the ecoinvent 3.4 database with the system model “Allocation, cut-off by classification”, and the IPCC (2013) life cycle impact assessment methodology based on Global Warming Potential [50]. The IPCC method includes all greenhouse-gas emissions, which is in kg CO_2-equivalent [51]. Other environmental burdens are out of the scope of this research.

The Global Warming Potential is in CO_2-equivalent hence all greenhouse-gas emissions are included when we refer to CO_2-emissions. We include net imports from neighbouring countries to determine the average import emission factor. The imports shares are based on the total annual imports for the year 2014–2015 from Austria (20.8%), Germany (40.8%), France (35.5%) and Italy (2.9%) [52]. For simplicity, we assume perfect prediction of CO_2-emissions in the multi-objective functions. Otherwise, the prediction is based on earlier developed hourly CO_2-emissions which could be unrealistic.

The CO_2-emission factors for the production of the battery technologies are presented in Table 1. The operation and production phase of batteries are considered in LCA foreground processes. End-of-life burdens are only considered in background LCA processes hence are not included in LCA foreground processes, due to the complexity of the end-of-life phase of batteries [53].

4.3. Electricity market

Market prices of the SwissIX market are obtained from EPEX [54]. The SwissIX day-ahead market prices are cleared the day before at 11.00, to represent market wholesale prices for the next day. In this work, the focus is on the intra-day market. Annual intra-day market prices are not freely available. Abrell [55] analyzed the Swiss intra-day market prices for different years and demonstrated that intra-day market prices in 2014 are on average 20.9% higher than day-ahead market prices. Therefore, the day-ahead market prices are multiplied with this factor to estimate the intra-day market prices.

Energy traders (e.g. aggregators) must trade a minimum amount of 0.1 MW power on the Swiss wholesale market [55]. Most CES systems could supply this minimum amount of power. However, it is not realistic that the proposed CES system can offer this amount of power individually for different reasons, such as constraints on the demand side of the community. Therefore, it is assumed that the aggregator owns multiple CES systems. In this way, the aggregator can pool the CES units and offers at least the minimum amount of power required to trade in the SwissIX spot markets. Swiss imbalance prices are identified which serves as an input in the multi-objective function in phase II (see Eqs. (21)). Imbalance prices are obtained from Swissgrid [56] for the year 2014–2015. Electricity is usually traded each 15 min in the Swiss intra-day market. However, our datasets are at hourly frequency hence we assume hourly electricity trading and imbalance pricing.

4.4. Load, generation and price prediction

Prediction of loads, PV generation and prices is required to estimate their values at timeslot $t-1$ at gate closure. In this work, a simple Seasonal Auto Regressive Integrated Moving Average (SARIMA) model is used to predict the bid of the aggregator to the TSO. SARIMA models include time correlations, randomness and seasonality of a dataset. In addition, SARIMA models are widely used to determine future electricity prices [57], PV generation [58] and demand loads [59–61].

Next, grid search is used to determine the best SARIMA fit, based on the Akaike Information Criterion (AIC), to our datasets. Grid search means that the SARIMA parameters are varied between 0 and 1. The SARIMA model contains non-seasonal and seasonal parameters in our datasets. We refer to Weron [57] for more elaboration on the different parameters of the SARIMA model. AIC is used to obtain the best fit of the SARIMA parameters to our datasets since AIC is able to measures the statistical fit of a model [62]. Ultimately, the best combination of parameters in SARIMA is selected per dataset. This is done when the combination of SARIMA parameters show the lowest AIC values.

In this work, the cyclic period of data (i.e. seasonality) is set to 24 h since the datasets demonstrate daily fluctuations. For example, PV generation, demand loads and electricity prices all show a daily pattern in our datasets. The SARIMA model parameters fitting starts one week before (i.e., seven cyclic periods) and continues until the end of the assessment period. This is sufficient to have good tuning of the model parameters as the minimum historical data needed in SARIMA is typically two full cyclic periods of data (i.e., two days) [63]. After choosing the best fit of the parameters (i.e., by making use of grid search and AIC) the model can be used to predict future values.

We are aware of better prediction models (e.g. see [64]). However, the SARIMA model is easy to implement. In addition, our main purpose of using SARIMA is to make a realistic economic and environmental

[2] The year 2010 is used as assessment year for CO_2-emissions since the year 2014 is not available in the STEM.

assessment while considering imbalance costs, instead of assuming a perfect knowledge of the input data and neglecting imbalance costs.

4.5. Grid

We assume a maximum allowed of grid absorption or injection of 8 kW per household [13], which corresponds to a community power of 176 kW ($P_{grid,max}$). The transformer capacity is indicated at 2.2 kW per household. This is the minimum installed capacity for Swiss households, situated in urban areas scenario [65]. This results in a total transformer capacity of 48.4 kW for our case study. Powers above this capacity (i.e. 48.4 kW or more, due to excess demand of electricity) or below (i.e. −48.4 kW or less, due to excess supply of electricity) could result in grid contingencies. The general models input parameters are described in Table 2.

4.6. CES battery

Different battery technologies are considered (see Section 1) and are described in more detail in [29]. A power to storage ratio of 1:2 is used for the CES battery. We examine a medium required battery share size of 7.5 kWh per household. This leads to a required CES capacity of 165 kWh. However, we expect that the battery size has a significant influence on the economic performance of battery technologies. Therefore, the required battery capacity size is varied in the sensitivity analysis. General and technology specific input parameters are presented in Table 1 for the medium sized CES battery. The installed battery sizes ($C_{bat,CES}$) are determined with Eq. (1).

5. Performance indicators

Performance indicators are essential to compare the EA and EA-PS scenarios, and the different battery technologies. The performance indicators are developed and applied from the perspective of the CES owner. After the optimization, the annual costs (c_{annual}) and annual CO_2-emissions (g_{annual}) from the multi-objective optimization can be determined with Eqs. (24) and (25).

$$c_{annual} = \sum_{t=1}^{8760} \left(c^t p^t_{grid,absI} \Delta t + c^t_{short} p^t_{short} \Delta t \right). \tag{24}$$

$$g_{annual} = \sum_{t=1}^{8760} g^t p^t_{grid,absII} \Delta t. \tag{25}$$

The following performance indicators are proposed.

5.1. System performance

5.1.1. Photovoltaic self-consumption ratio (PVSC)

The main goal of the optimization problem is to minimize the costs and CO_2-emissions from grid absorption. This can be achieved by maximizing the consumption of self-produced PV electricity in the community since it is assumed that the CO_2-emissions and costs of PV electricity are zero. Consequently, the following indicator is essential to compare the different alternatives on the ability to consume self-produced PV generation. The PVSC ratio is always between 0 and 1, and closer to 1 means a higher self-consumption ratio of the system.

$$PVSC = \frac{\sum_{t=1}^{8760} \left(P^t_{PV} - p^t_{grid,inj} \right)}{\sum_{t=1}^{8760} P^t_{PV}}. \tag{26}$$

5.1.2. Incidents

The following system performance indicator is used to determine the share of potential incidents of the total grid interactions. In this work, a potential incident is indicated as exceeding the capacity of the distribution transformer by grid absorption or grid injection. Exceeding the transformer capacity could result in system contingencies on the distribution level with outages as a consequence. Therefore, this indicator is of high importance for the DSO, since the DSO is responsible for a reliable operation at the distribution level. The share of potential annual incidents (I_{share}) is obtained with Eq. (27).

$$I_{share} = \frac{\sum_{t=1}^{8760} \left[p^t_{grid,absII} \geqslant P_{trans} \right] + \sum_{t=1}^{8760} \left[p^t_{grid,inj} \geqslant P_{trans} \right]}{\sum_{t=1}^{8760} \left[p^t_{grid,absII} > 0 \right] + \sum_{t=1}^{8760} \left[p^t_{grid,inj} > 0 \right]}, \tag{27}$$

where [...] are the Iverson brackets which give "1" every time-step the condition between the bracket is true and "0" otherwise.

5.2. Economic indicators: Profitability

5.2.1. Imbalance costs

The annual imbalance costs ($C_{imbalance}$) determine the costs the CES owner should pay to the TSO when the actual grid absorption (in phase II) is higher than the grid absorption in the energy bid (in phase I).

$$C_{imbalance} = \sum_{t=1}^{8760} c^t_{short} p^t_{short} \Delta t. \tag{28}$$

5.2.2. Annual revenue, costs and profits

Three types of revenue streams are included to determine the total annual revenue (R_{annual}). First of all, some revenue can be obtained when less electricity is consumed at t than earlier scheduled in the bid at $t-1$. In this way, the aggregator receives the "long" price at t. Therefore, the amount of "long" imbalance power is determined (P^t_{long}).

$$P^t_{long} = \begin{cases} p^t_{grid,absII} - p^t_{grid,absI} < 0 \ : \left| p^t_{grid,absII} - p^t_{grid,absI} \right|, \\ p^t_{grid,absII} - p^t_{grid,absI} \geqslant 0 \ : 0. \end{cases} \tag{29}$$

Secondly, the largest revenue obtained from the CES system is by selling electricity to the community for the residential electricity price (c^t_{hh}), corresponding to the community aggregated demand profile. Furthermore, the second term in Eq. (30) refers to the additional revenue that can be made from grid injection, when electricity cannot be directly consumed or stored in the CES battery. In this way, grid injection is remunerated with the "long" price at t.

Table 2
General input parameters.

General	Value	Unit
Community power demand	201[a]	MWh/year
Community PV generation	67.7[a]	MWh/year
Battery		
SoC_0	50	%
$P_{bat,max}$: $C_{bat,req}$	1:2	–
$C_{bat,req}$	165	kWh
Grid		
$P_{grid,max}$	176	kW
S	1	kW
P_{trans}	48.4	kW
BEV		
P^a_{min}	0	kW
P^a_{max}	1.4	kW

[a] For the year 2014–2015.

$$R_{annual} = \sum_{t=1}^{8760} \left(c_{hh}^{t} \left(p_{sl}^{t} + P_{nsl}^{t} \right) \Delta t + c_{long}^{t} p_{grid,inj}^{t} \Delta t + c_{long}^{t} P_{long}^{t} \Delta t \right). \quad (30)$$

Next, the total annual costs can be calculated by summing the annual operation costs and maintenance costs ($c_{maintenance}$). Furthermore, the third term includes remuneration of PV electricity generation to residential customers in the form of a FiT ($c_{paid,PV}^{t}$). This leads to the following equation to indicate the total annual costs (C_{annual}).

$$C_{annual} = c_{annual} + c_{maintenance} + \sum_{t=1}^{8760} c_{paid,PV}^{t} P_{PV}^{t} \Delta t. \quad (31)$$

Next, the total annual benefits/profits (B_{annual}) can be calculated by the following (simple) equation.

$$B_{annual} = R_{annual} - C_{annual}. \quad (32)$$

5.2.3. LCOE & PBP

In addition, the Levelized Costs Of Electricity (LCOE) and the simple Pay Back Period (PBP) are defined to compare the performances of the EA and EA-PS scenarios, and the different battery technologies. We assume a system lifetime of 12 years and use a discount rate of 5% [29].

With the LCOE, the costs per unit electricity delivered to the end-user customer is determined. The LCOE includes the system operation, investment and Operation and Maintenance (O&M) costs of the CES battery.

$$LCOE = \frac{I_{CES} + \sum_{l=1}^{L} \left(C_{annual}/(1+\gamma)^{l} \right)}{\sum_{l=1}^{L} \left(\sum_{t=1}^{8760} \left(p_{sl}^{t} + P_{nsl}^{t} \right)/(1+\gamma)^{l} \right)}, \quad (33)$$

where I_{CES} are the investment costs in the CES battery [euro], γ is the interest rate [%] and L is the lifetime of the system [years].

Furthermore, the simple PBP is used to determine the number of years before the initial investment is recovered.

$$PBP = \frac{I_{CES}}{B_{annual}}. \quad (34)$$

6. Results

We generate the results for the two scenarios (i.e., EA and EA-PS) and the six battery technologies, assuming equal weighting of costs and CO_2-emissions, in Sections 6.1–6.4. Next, the sensitivity analysis, based on different FiT remuneration rates and required battery storage sizes, is presented in Section 6.5. After that, results based on different costs and CO_2-emission weighting are presented using the Pareto frontier method in Section 6.6.

6.1. Operation

6.1.1. Energy Arbitrage scenario

The results obtained from the optimization model for the EA scenario are presented in Table 3. The highest energy throughputs (i.e. battery charge and discharge) are obtained from the NCA-LTO, LFP-C and NMC-C batteries since these batteries have a comparatively long cycle lifetime and Roundtrip Efficiency (RE). In contrast, the energy throughput of the NCA-C battery is the lowest between LiBs since we assume that the battery lifetime of each battery must be respected to reduce investment costs by additional battery pack replacements. Therefore, the NCA-C battery is constrained in the battery operation. This can be explained by the comparably low number of cycles (i.e. 2498 cycles) of the NCA-C battery. In addition, the VRLA battery and the VRFB consume a higher amount of grid electricity, which is needed to compensate for the low RE of these batteries.

Furthermore, the PVSC is the highest for the VRFB (i.e. PVSC of approximately 1). In the VRFB, more PV electricity is lost by the charging and discharging process (i.e., lowest RE = 66%, see Table 1). As a consequence, this results in a higher PVSC and a lower grid injection. This is also demonstrated in the PVSC of the other batteries. For example, the NCA-LTO battery has the lowest PVSC since this battery has the highest RE. These examples demonstrate that a high PVSC does not always represent the best performance on the PVSC indicator.

Moreover, there is no grid constraint implemented for grid absorption in the EA scenario. In this way, the maximum battery power is the same as the rated battery power ($P_{bat,max}$), which inevitably results in large grid absorption/injection peaks (see Section 6.4). Consequently, the shares of potential incidents is large for all battery technologies. The largest share of incidents are obtained from the NCA-LTO, LFP-C and NMC-C batteries. These batteries offer a high number of cycles during the system lifetime. Therefore, the battery degradation constraint is more relaxed on these battery technologies hence this results in more cycles and potential incidents.

6.1.2. Energy Arbitrage - Peak Shaving scenario

In this section, the results from the EA-PS scenario are discussed. Only the differences with the EA scenario are explained to avoid repeated statements. Table 4 demonstrates that the operation parameters are slightly changed. The share of potential incidents are reduced to zero for all batteries, since we implemented a constraint on grid electricity absorption and grid injection (see Eqs. (22) and (23)). Also, the implemented constraints result in less battery utilization which is demonstrated in lower charging and discharging values for all battery technologies. In this way, less power can be absorbed during timeslots with low electricity prices and/or low CO_2-emissions from the grid.

6.2. Economic indicators

6.2.1. Energy Arbitrage scenario

The economic performance of the EA scenario is presented in Table 5. It turns out that all LiBs and the VRFB show a profitable system design since the PBPs of these batteries are lower than the system lifetime (assumed to be 12 years). The lowest PBP (6.83 years) and LCOE (0.126 euro/kWh) is obtained from the NMC-C battery, followed by the NCA-LTO battery and LFP-C battery, respectively. The best economic performance of the NMC-C battery can be (mainly) explained by the low operation and investment costs. The NMC-C battery can offer a comparably high amount of cycles with low investments costs.

The best operational performance is obtained from the NCA-LTO battery due to the high RE (91%) of this battery technology. However,

Table 3
Annual results on different performance indicators for the EA scenario.

	NMC-C	LFP-C	NCA-C	NCA-LTO	VRLA	VRFB	Unit
Power injected	901	802	901	1006	262	33	kWh
Power absorbed	144,114	146,711	142,936	143,408	155,322	162,473	kWh
Battery charge	86,729	94,124	76,023	96,991	85,551	84,610	kWh
Battery discharge	77,282	81,981	67,753	88,354	64,256	55,935	kWh
Incidents	0.254	0.297	0.201	0.321	0.220	0.200	–
PVSC	0.987	0.988	0.987	0.985	0.996	1.000	–

Table 4
Annual results on different performance indicators for the EA-PS scenario.

	NMC-C	LFP-C	NCA-C	NCA-LTO	VRLA	VRFB	Unit
Power injected	901	802	901	1006	262	33	kWh
Power absorbed	143,076	144,506	142,936	141,665	153,358	160,874	kWh
Battery charge	77,295	77,168	76,023	77,624	77,696	79,906	kWh
Battery discharge	68,885	67,229	67,753	70,730	58,365	52,831	kWh
Incidents	0	0	0	0	0	0	–
PVSC	0.987	0.988	0.987	0.985	0.996	1.000	–

the investment costs of the NCA-LTO are comparably high which results in the second best economic performance. The LFP-C and NCA-C batteries perform moderate due to their relatively high investment costs. For example, the NCA-C battery needs more than one battery pack replacement (see Table 1) during the system lifetime, which increases the investment costs of this battery technology. The VRFB performs comparatively worse due to the high O&M costs and the low RE (66%) of this battery technology.

The VRLA battery demonstrates a non-profitable system design with a high PBP of 26.4 years due to its high investment and operation costs. This can be explained by the large oversizing which is needed to compensate for the low RE and low DoD of this battery. In addition, the VRLA battery has a low battery lifetime (4.1 years), which requires almost three battery pack replacement during the system lifetime (see Table 1). These battery pack replacements are needed to offer the annual number of cycles for the EA application (i.e., 365 cycles per year).

The imbalance costs are relatively low and comparable between all battery technologies, with a share of 1–2% of the total annual costs. The low imbalance costs can be explained by the low Swiss imbalance prices. Note that we oversized the batteries and include a high number of annual cycles for the EA application to increase the comparability between battery technologies. This choice results in small differences between battery technologies. The lowest imbalance costs are obtained from the NCA-LTO battery since this battery has the best operational performance. Remarkably, the VRLA battery has relatively low imbalance costs, while this battery has a low DoD and RE. This can be explained by our choice to oversize the batteries and to include additional battery pack replacements. This partly compensates the poor technology characteristics of the VRLA battery however leads to high investment costs.

6.2.2. Energy Arbitrage - Peak Shaving scenario

The economic results for the EA-PS scenario are presented in Table 6. It turns out that the economic performance is slightly reduced for most batteries. Interestingly, these results emphasize that the differences with the EA scenario are small. For example, the PBPs differ with a maximum of 0.06 years in comparison with the EA scenario. Note that both economic and environmental benefits can be obtained from grid deferral, but these are not included in our work (see discussions in Section 7).

Remarkably, the economic performance of the VRFB (i.e. higher annual profits) is slightly better in comparison with the EA scenario. This can be (mainly) explained by smaller prediction errors (i.e. imbalance costs) due to power boundaries on grid absorption and injection. This results in lower imbalance power (p^t_{short}) hence lower imbalance costs. Furthermore, there are sufficient other timeslots where the intra-electricity price is low hence the battery can still be charged with low electricity prices.

6.3. Environmental indicators

6.3.1. Energy Arbitrage scenario

The results on the environmental indicators for the EA scenario are presented in Table 7. It turns out that the lowest operational CO_2-emissions are obtained from the NCA-LTO battery, followed by the NMC-C and LFP-C battery, respectively. The NCA-LTO has the highest RE, which results in lower absorption of electricity from the grid hence lower CO_2-emissions. The VRLA battery and VRFB perform worse due to the low REs of these battery technologies. The results are fundamentally changed when the production phase is included.

In this case, the best environmental performance is obtained from the NMC-C battery, followed by the LFP-C and NCA-LTO battery, respectively. The NMC-C battery performs comparatively good on both operation and production. In contrast, the CO_2-emissions of battery production for the NCA-LTO battery are comparably high (see Table 1). This explains the moderate performance of the NCA-LTO battery on lifetime CO_2-emissions. The results demonstrate that the VRLA battery shows the highest CO_2-emissions. This can be explained due to the required battery pack replacements and the large oversizing of this battery technology.

6.3.2. Energy Arbitrage - Peak Shaving scenario

Table 8 demonstrates that the environmental performance of the EA-PS scenario is slightly worse in comparison with the EA scenario. More CO_2-emissions are produced with the EA-PS scenario, since the battery must be charged with more carbon-intensive grid electricity. However, the differences of the total CO_2-emissions with the EA scenario are small since the annual CO_2-emissions are slightly increased with only 2–5%. Again, the NMC-C battery performs best, followed by the LFP-C and NCA-LTO batteries, when the lifetime is included.

Table 5
Annual results on different economic indicators for the EA scenario. Investment, PBP and LCOE are based on the system lifetime.

	NMC-C	LFP-C	NCA-C	NCA-LTO	VRLA	VRFB	Unit
Investment[a]	94,394	125,253	131,467	117,166	348,178	117,863	euro
Operational costs	7232	7326	7254	7144	7847	8275	euro/year
Total annual costs	14,740	14,834	14,762	14,651	15,355	18,588	euro/year
Revenue	28,564	28,563	28,560	28,568	28,565	28,574	euro/year
Imbalance costs	239	237	263	238	244	265	euro/year
PBP	6.83	9.12	9.53	8.42	26.36	11.80	years
LCOE (γ = 5%)	0.126	0.144	0.147	0.138	0.271	0.158	euro/kWh
Profit	13,824	13,729	13,798	13,916	13,210	9986	euro/year

[a] Investment costs and CO_2-emissions from battery production are normalized to the system lifetime to include possible battery pack replacements.

Table 6
Annual results on different economic indicators for the EA-PS scenario. Investment, PBP and LCOE are based on the system lifetime.

	NMC-C	LFP-C	NCA-C	NCA-LTO	VRLA	VRFB	Unit
Investment[a]	94,394	125,253	131,467	117,166	348,178	117,863	euro
Operational costs	7308	7379	7302	7235	7853	8246	euro/year
Total annual costs	14,816	14,887	14,810	14,743	15,361	18,559	euro/year
Revenue	28,562	28,558	28,560	28,560	28,555	28,558	euro/year
Imbalance costs	182	177	178	183	167	178	euro/year
PBP	6.87	9.16	9.56	8.48	26.39	11.79	years
LCOE (γ = 5%)	0.126	0.144	0.147	0.139	0.271	0.158	euro/kWh
Profit	13,746	13,671	13,749	13,816	13,194	9998	euro/year

[a] Investment costs and CO_2-emissions from battery production are normalized to the system lifetime to include possible battery pack replacements.

6.4. Shift to all-electric energy systems

6.4.1. Energy Arbitrage scenario

Fig. 4 demonstrates the system operation of the CES system ($C_{bat,req}$ of 165 kWh) during a winter week for the EA scenario with the same weighting of costs and CO_2-emissions in the multi-objective function. The left figure shows the weekly charging and discharging pattern during a winter week with PV generation. The initial load is presented in the right figure in order to compare the difference in loads between the all-electric scenario and the initial scenario. Note that there is no electric heating, PV array installed and BEV used in the initial scenario.

The left plot of Fig. 4 reveals that the battery is often charged with the maximum battery power in order to charge during PV generation times, low grid electricity prices and/or low grid CO_2-emissions. In addition, the transformer load is presented in the right plot of Fig. 4. This figure clearly visualizes that unconstrained charging of a CES battery results in large grid absorption peaks in an all-electric scenario during a winter week. At certain times, the load on the distribution transformer is higher than the installed capacity of the transformer in the distribution network. Note that this could results in system contingencies. Therefore, the shift to all-electric energy systems could become problematic when no power constraint is added for the distribution transformer capacity.

Fig. 5 shows the system operation during a summer week for the EA scenario. The left plot reveals that there is more PV electricity generation due to higher solar irradiation. At the 24th of July, some PV electricity has to be injected into the electricity grid since the battery is fully charged. The right figure shows that less electricity is absorbed compared to the winter week. This can be explained due to higher self-sufficiency of the CES system as a result of higher PV electricity generation. Consequently, this results in a lower number of potential incidents with the transformer compared to the winter week.

6.4.2. Energy Arbitrage - Peak Shaving scenario

Fig. 6 demonstrates the EA-PS scenario during a winter week. Note that the charging and discharging peaks of electricity absorption are still visible. However, the right figure clearly visualizes that the capacity of the transformer in the distribution network is respected during this winter week. The community load is never higher than the transformer capacity. Note that the implementation of a constraint for peak shaving could result in the scheduling of demand loads to timeslots with higher electricity prices or higher CO_2-emissions. This could lead to a less beneficial economic and/or environmental performance, as demonstrated in Sections 6.2 and 6.3.

Fig. 7 shows the system operation during a summer week for the EA-PS scenario. Again, this figure demonstrates that the transformer capacity is never reached.

6.5. Sensitivity analysis

We only select the EA-PS scenario for the sensitivity analysis, since the differences between the EA and EA-PS scenario are small. Furthermore, the combination of these applications shows promising economic and environmental potential.

6.5.1. Feed-in-Tariff

The relation between FiT remuneration and the PBPs are demonstrated in Fig. 8. This figure shows that most battery technologies have a profitable system design, even with a high FiT remuneration for PV generation. Remarkably, the VRLA is never profitable due to high investment costs. Furthermore, the PBPs and profitability of the CES owner can be increased when the FiT, paid to residential households, is reduced. On the other hand, a lower FiT could result in non-participation of households in the CES system. This could result in a lower PV supply hence higher operation costs and higher CO_2-emissions from the grid.

6.5.2. Required CES storage size

We assumed a required storage capacity size of 7.5 kWh per household, which leads to a required community storage size of 165 kWh. The required storage size is varied in Fig. 9. The PBPs are reduced when the required storage size is decreased. This can be explained by the high investments costs for battery technologies. These results demonstrate that a larger battery cannot benefit sufficiently from a better system operation with current battery costs.

6.6. Pareto frontiers

6.6.1. Motivation

The Pareto frontier approach is a well-known method that is typically used to analyze the trade-off in optimization problems with multiple objectives. A point is considered a Pareto optimal when no further Pareto improvements can be made in each of the considered multiple objectives [66]. For instance, if the multiple objectives are

Table 7
Results on different environmental indicators for the EA scenario. Annual emissions only includes operational CO_2-emissions. "Annual & production" is based on operation and also includes normalized CO_2-emissions from the production phase. Battery production is based on the system lifetime.

	NMC-C	LFP-C	NCA-C	NCA-LTO	VRLA	VRFB	Unit
Annual	6619	6661	6744	6497	7208	7615	kg CO_2/year
Annual & production	9170	9429	11,487	10,411	15,706	10,499	kg CO_2/year
Battery production[a]	30,610	33,219	56,912	46,967	101,981	34,606	kg CO_2

[a] Investment costs and CO_2-emissions from battery production are normalized to the system lifetime to include possible battery pack replacements.

Table 8
Results on different environmental indicators for the EA-PS scenario. Annual emissions only includes operational CO_2-emissions. "Annual & production" is based on operation and also includes normalized CO_2-emissions from the production phase. Battery production is based on the system lifetime.

	NMC-C	LFP-C	NCA-C	NCA-LTO	VRLA	VRFB	Unit
Annual	7011	7090	7020	6934	7600	8080	kg CO_2/year
Annual & production	9561	9858	11,763	10,848	16,098	10,964	kg CO_2/year
Battery production[a]	30,610	33,219	56,912	46,967	101,981	34,606	kg CO_2

[a] Investment costs and CO_2-emissions from battery production are normalized to the system lifetime to include possible battery pack replacements.

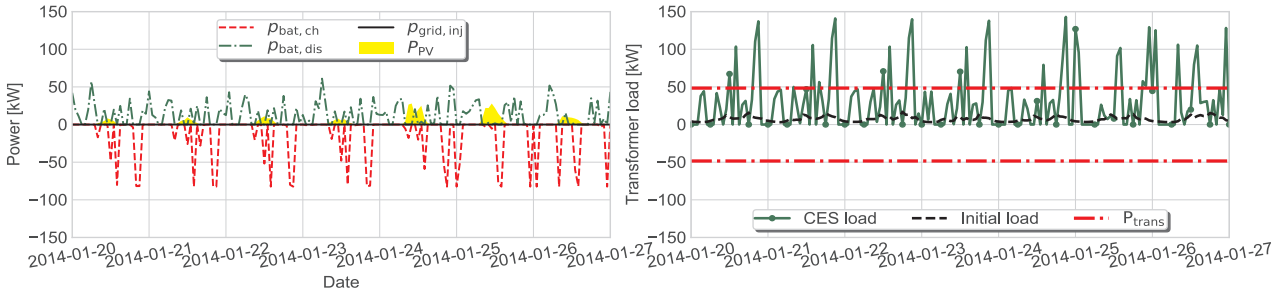

Fig. 4. System operation during a winter week for the EA scenario.

minimization of electricity costs and CO_2-emission, a point is Pareto optimal if there is no other point whose electricity costs and CO_2-emission are no worse. Pareto frontiers approaches have been widely used to analyze the trade-off in different multi-objective problems in this area of research, such as economic and emission dispatch problems [67–69], economic and environmental appliances scheduling [70], distribution feeder reconfiguration [71], low-emission cost-effective dwellings with HVAC systems [36] and day-ahead energy resource scheduling [21].

In this section, we present the Pareto-frontiers of the two objectives considered in this study (i.e., f_1 and f_2, mentioned in Section 3) to analyze how the economic an environmental assessment of CES, in the two scenarios and for each of the six considered battery technologies, differ when using different costs and CO_2-emission weighting in the multi-objective problem. We use the weighting method [72] as a posteriori method so that different weights of the two objectives are used to generate different Pareto optimal solutions and then the aggregator can select the most satisfactory combination of the weights based on the achieved results. Practically, these Pareto frontiers are generated by repeating the multi-objective optimization problem for different combinations of weighting for costs (i.e. w_1) and CO_2–emissions (i.e. w_2) and each run produces one Pareto optimal solution.

6.6.2. Energy Arbitrage scenario

Fig. 10(a) and (c) show the trade-offs of the EA scenario between costs and CO_2-emissions for each battery technology during system operation and per lifetime year (i.e., by including the production phase), respectively. Note that the bandwidth of each battery technology demonstrates the optimized values for a specific set of weighting for costs (i.e. w_1) and CO_2-emissions (i.e. w_2). For example, when the weigh of costs is set to 0.6, the weigh of CO_2-emissions is set to 0.4.

Firstly, these Pareto frontiers demonstrate that the results change significantly when the optimization is based on costs or CO_2-emissions only (i.e. the two end points of each frontier). For most battery technologies, a large amount of CO_2-emissions can be avoided with relatively low costs. For example, with the NMC-C battery, annual CO_2-emissions can be reduced with approximately 8 ton for an additional 1000 euros per year.

Furthermore, these figures reveal that LiBs have the lowest costs and CO_2-emissions during system operation. The best economic and environmental performance during operation is obtained from the NCA-LTO battery. However, the differences with the NMC-C and LFP-C batteries are small. Furthermore, the VRFB and VRLA battery perform worse during system operation, which (again) can be explained by the low RE of these batteries.

The results are changed when the production phase is included (see Fig. 10(c)). In this case, the best economic and environmental performance is obtained from the NMC-C battery. Furthermore, all LiBs demonstrate good economic and environmental performance. The VRFB performs relatively worse on economic performance. This can be explained due to the high costs of the energy storage unit and the power generation unit. These results clearly demonstrate that the VRLA battery performs worst on both economic and environmental performance.

6.6.3. Energy Arbitrage - Peak Shaving scenario

Fig. 10(b) and (d) show the Pareto frontiers for the EA-PS scenario during system operation and per lifetime year by including the production phase, respectively. As mentioned earlier, all battery

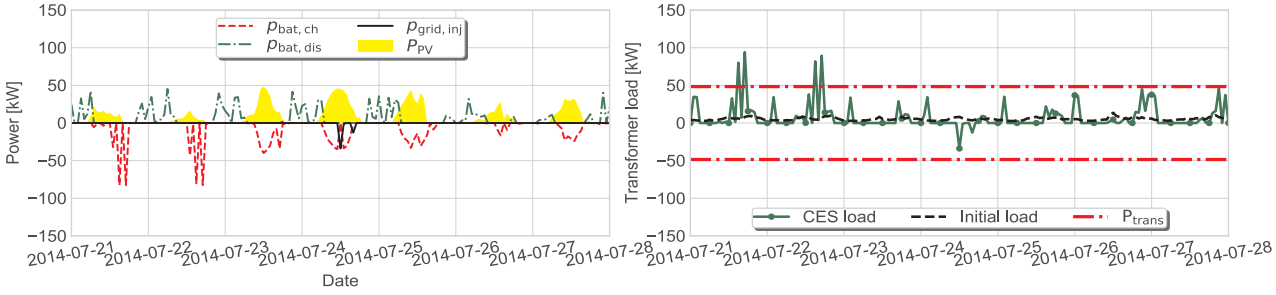

Fig. 5. System operation during a summer week for the EA scenario.

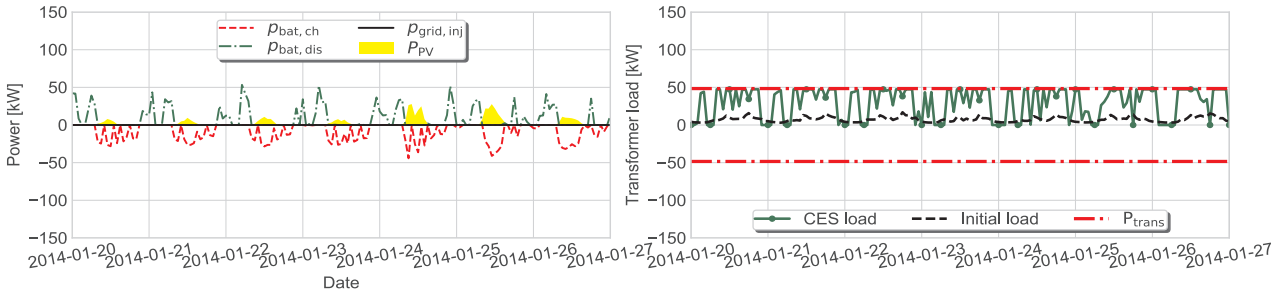

Fig. 6. System operation during a winter week for the EA-PS scenario.

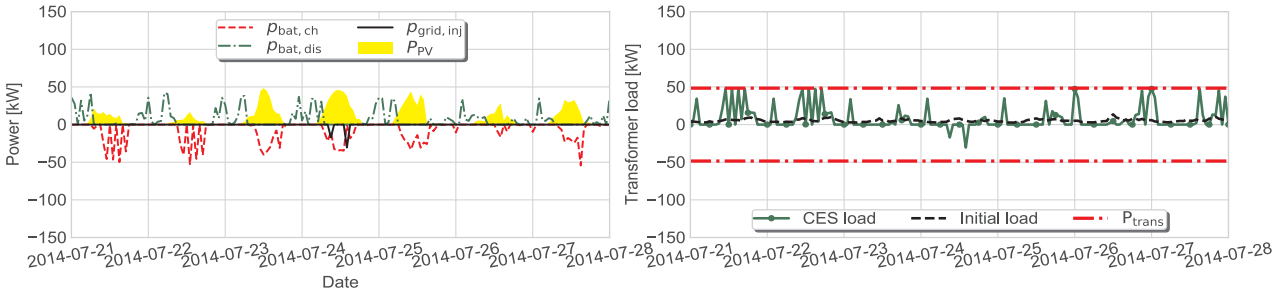

Fig. 7. System operation during a summer week for the EA-PS scenario.

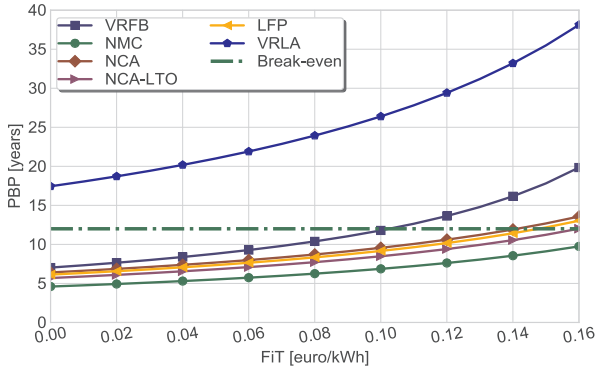

Fig. 8. Relation between the FiT remuneration for PV generation and the PBPs for all battery technologies for the EA-PS scenario.

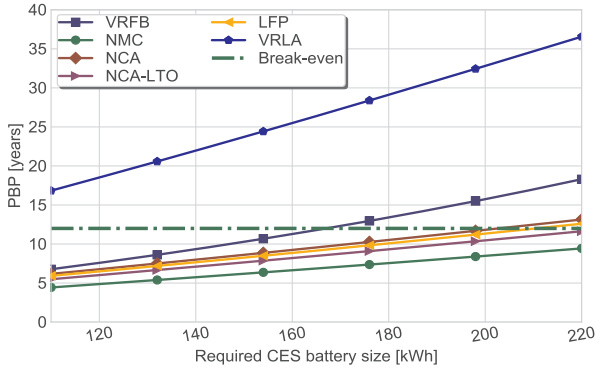

Fig. 9. Relation between required CES battery ($C_{bat,req}$) size and PBP for all battery technologies for the EA-PS scenario.

technologies perform slightly worse on both costs and CO_2-emissions. Moreover, the bandwidth (i.e. range of cost and CO_2-emission values) of the optimization values is reduced due to the implemented constraints on power boundaries of grid absorption and injection. Again, the differences between the EA scenario and the EA-PS scenario are small.

7. Discussions

Firstly, only battery investment costs are included in the investment costs. However, additional EMSs are required to schedule and optimize the loads of each household individually. These investments are not included in our work since it is uncertain if the CES owner or the household should pay for these EMSs. PBPs of EMSs are in between the range of 0.7–1.8 years [73] hence this could result in a slightly less beneficial economic and environmental performance of the scenarios presented in our work.

Also, the cost and environmental assessment should be specified on the preferences of the CES owner. For example, a CES owner could choose to give higher importance to costs or CO_2-emissions. This economic or environmental preference results in an optimal point in the Pareto frontier for each battery technology, hence the best battery technology can be chosen [66]. Therefore, the choice of the best compromise solution and best battery technology depends on the purpose and strategy of the CES owner. On the other hand, our results demonstrate that the NMC-battery performs best on all cost and CO_2-emission weightings on a lifetime basis. However, the performance could be different with other battery applications.

For simplicity, we started with equal weighting of costs and CO_2-emissions. However, the two objectives have different units (i.e. costs and CO_2-emissions) hence may not reflect equal importance of the two objectives. Therefore, more detailed focus on weighting of the two objectives can be given. On the other hand, we generated Pareto frontiers to identify the performance on all different cost and CO_2-emission weightings. Furthermore, the optimization problem can be extended by including additional constraints for the distribution network, BEV and shiftable appliances. However, this could lead to higher complexity of the optimization algorithm, hence longer computation times. This could also require the use of different methods for the multi-objective optimization problem formulation and different algorithms for finding the optimal solution and Pareto frontiers. Besides, it could be interesting to assess different scales of the proposed system design to determine the optimal system design for CES systems.

Furthermore, we developed a case study from the perspective of an aggregator and a DSO, where we expected that each household participate by delivering their PV electricity generation to the CES system. In reality, this could be more complex since households can decide to

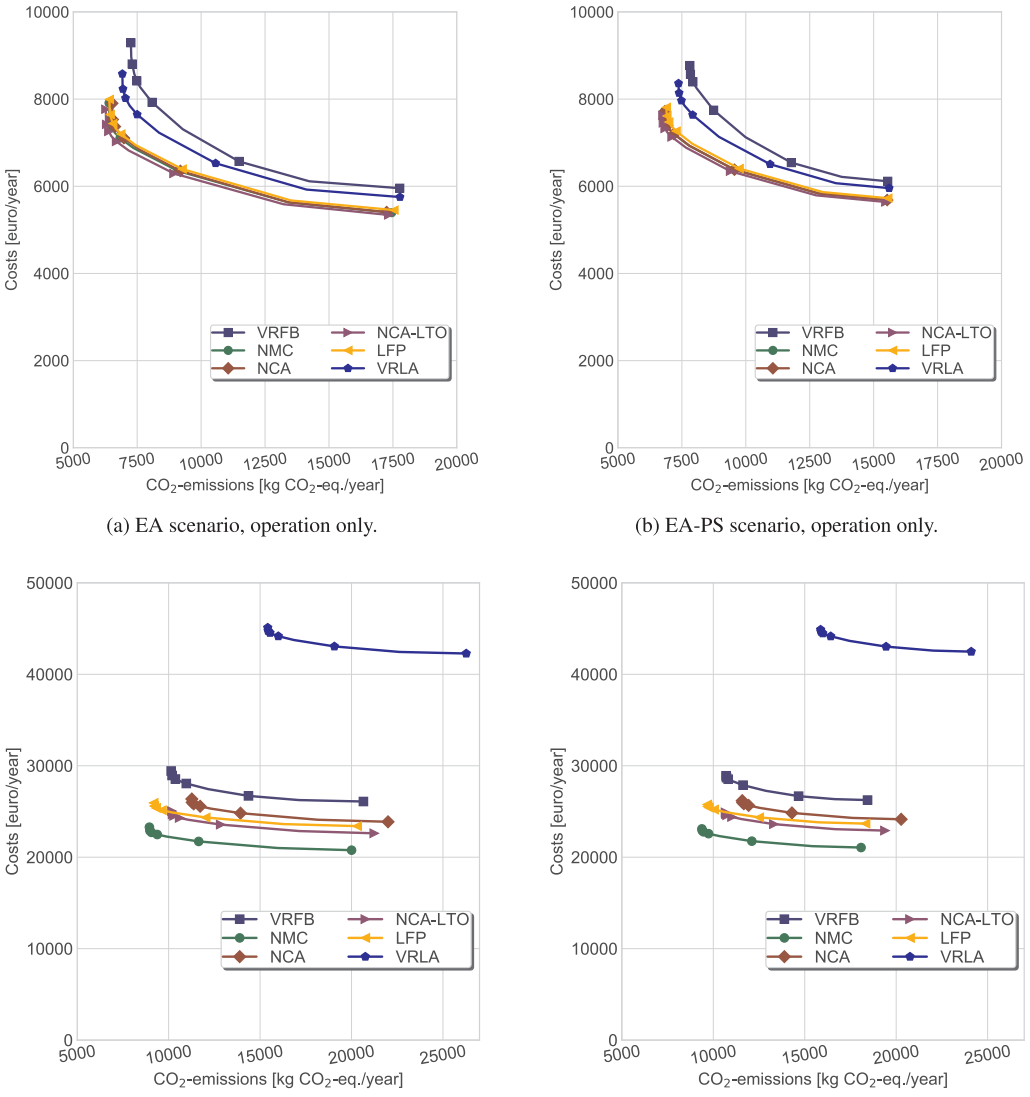

(a) EA scenario, operation only.

(b) EA-PS scenario, operation only.

(c) EA scenario, including production.

(d) EA-PS scenario, including production.

Fig. 10. Pareto frontiers of CO_2-emissions and costs for the two scenarios, during operation and including production, and for a required CES battery size of 165 kWh ($C_{bat,req}$).

refuse the adoption of a PV installation [74]. Therefore, pilot projects and real case studies should be implemented to test different business models.

We applied our MILP model on one case study only. The model requires testing on more and different case studies before the results can be generalized. For example, different aggregated demand loads and PV generation profiles as well as battery sizes can be implemented. This could result in different economic and environmental performance of battery technologies and applications. Also, the system design could integrate other storage technologies, such as heat storage (see [13]).

In addition, we only considered the BEVs as shiftable loads. However, more flexible loads (e.g. heat pumps and washing machines) can be included. This could result in lower operational costs and CO_2-emissions since more load can be shifted to lower electricity and/or CO_2-emission times. In addition, we only consider CO_2-emissions as environmental indicator. However, other environmental indicators could be included to give a wider assessment of environmental impacts [34].

Furthermore, we used simplified assumptions of the bid process in the Swiss intra-day market. In reality, the bid process is more complex since it depends on many other factors. For example, it is uncertain if the bid is accepted. Therefore, the analysis of the bid phase and the determination of imbalance costs could be improved to increase the reliability of the economic and environmental assessment. Furthermore, we assumed that the intra-day market prices are higher with a specific percentage than the day-ahead market prices (i.e., Swiss intra-day market prices were not freely available). In reality, intra-day market prices are usually more volatile than day-ahead market prices hence the results could be slightly different when using real intra-day electricity prices.

Also, we decided to predict the aggregated demand load, PV generation and electricity prices based on a simple prediction model. Therefore, the prediction at timeslot $t-1$ can be improved which could reduce imbalance costs. On the other hand, our results demonstrate that the imbalance costs have a relatively small share of the annual operation costs and are of low importance in our assessment. This can be explained by the low imbalance electricity prices in the Swiss electricity market. Furthermore, the flexibility of the CES system can be used to reduce imbalance costs. For example, electricity can be charged or discharged to compensate wrong predictions submitted in the energy bid. For instance, if Swiss TSOs decide to increase imbalance prices, more benefits can be obtained with a larger storage capacity in order to

reduce imbalance costs of the energy bid. In this way, higher imbalance prices could stimulate the adoption of ESSs.

Besides peak shaving, other applications can be implemented to reduce the system costs of CES deployment [16]. For example, CES could deliver additional promising applications, such as area and frequency regulation [17]. Furthermore, the cost reduction obtained from grid deferral is not included in our EA-PS scenario since it is difficult to estimate the potential benefits from grid deferral. Currently, the costs and CO_2-emissions are increased in the EA-PS scenario when peak shaving is implemented. However, we expect that peak shaving provides additional benefits to the DSO hence this could result in a more beneficial business case for the EA-PS scenario.

8. Conclusions

This paper started with a strategy to minimize grid absorption, CO_2-emissions and imbalance costs of an aggregator operating in the Swiss intra-day market using a CES system. We examined two scenarios of CES ownership. The first scenario (i.e. EA scenario) was based on the individual ownership of the CES battery by an aggregator. The second scenario (i.e. EA-PS scenario) was based on a shared ownership between an aggregator and a DSO. These CES owners had different purposes with the CES system. The DSO aimed to avoid system contingencies by reducing the load on the distribution transformer by implementing peak shaving, while the aggregator aimed to minimize operation costs and CO_2-emissions by EA. A multi-objective MILP model was developed to minimize operation costs and CO_2-emissions in the two scenarios. This MILP model was tested on a community situated in Cernier (Switzerland), considering six battery technologies: NMC-C, LFP-C, NCA-C, NCA-LTO, VRLA and the VRFB.

The results demonstrate economic profitability for all LiBs (NMC-C, LFP-C, NCA-C and NCA-LTO) and the VRFB, for both the EA and EA-PS scenario. The EA scenario, where an aggregator owns the battery individually, shows a slightly better economic and environmental performance in comparison with the EA-PS scenario.

Furthermore, transformer stations turn out to be critical elements within the current infrastructure and will have to be reinforced for all-electric communities. Alternatively, we recommend to combine EA with PS to prevent potential problems related to the distribution transformer capacity when designing all-electric energy systems. Therefore, we recommend aggregators to collaborate with DSOs to prevent problematic loads on the distribution transformer while having a profitable business case with a good environmental performance.

Moreover, LiBs (e.g. NMC-C and NCA-LTO) perform best in the economic and environmental analysis. Therefore, we recommend to implement LiBs for CES deployment. More specifically, our results demonstrate that the NMC-C battery performs best on both economic and environmental performance.

Furthermore, the Pareto frontiers reveal that the economic and environmental performance of battery technologies is sensitive when applying different weighting of costs and CO_2-emissions. We believe that environmental impacts of systems and technologies will become more influential in the assessment of energy systems due to more aggressive climate policy. For that reason, we recommend to consider both costs and environmental impacts in the optimization of CES systems and (battery) technologies.

This paper demonstrates that additional benefits and profitability can be obtained when CES applications are combined. Therefore, future research should be directed into the integration of other storage technologies and applications of CES systems, considering both costs and additional environmental impact indicators.

Acknowledgements

This work was partially funded by the Joint Programming Initiative (JPI) Urban Europe project: “PARticipatory platform for sustainable ENergy managemenT (PARENT)”, the Netherlands Organization for Scientific Research (NWO) and the Commission for Technology and Innovation in Switzerland (CTI) within the Swiss Competence Centre for Energy Research in Heat and Electricity Storage (SCCER-HaE), contract number 1155000153.

References

[1] IEA. Status of power system transformation: advanced power plant flexibility. Tech rep. International Energy Agency, Paris; 2017. doi:https://doi.org/10.1787/9789264278820-en.
[2] IEA. Renewables 2017: analysis and forecasts to 2022 – executive summary. Tech rep. International Energy Agency; 2017. < https://www.iea.org/Textbase/npsum/renew2017MRSsum.pdf > .
[3] Sandhu M, Thakur T. Issues, challenges, causes, impacts and utilization of renewable energy sources - grid integration. J Eng Res Appl 2014;4(3):636–43.
[4] IRENA. Global energy transformation: a roadmap to 2050. Tech rep. International Renewable Energy Agency, Abu Dhabi; 2018.
[5] Verzijlbergh R, De Vries L, Dijkema G, Herder P. Institutional challenges caused by the integration of renewable energy sources in the European electricity sector. Renew Sust Energy Rev 2017;75:660–7. https://doi.org/10.1016/j.rser.2016.11.039.
[6] IEA. Smart grids in distribution networks. Tech rep. International Energy Agency, Paris; 2015.
[7] Katsanevakis M, Stewart RA, Lu J. Aggregated applications and benefits of energy storage systems with application-specific control methods: a review. Renew Sust Energy Rev 2017;75:719–41. https://doi.org/10.1016/j.rser.2016.11.050.
[8] Parra D, Swierczynski M, Stroe DI, Norman SA, Abdon A, Worlitschek J, et al. An interdisciplinary review of energy storage for communities: challenges and perspectives. Renew Sust Energy Rev 2017;79:730–49. https://doi.org/10.1016/j.rser.2017.05.003.
[9] Lampropoulos I, van den Broek M, van der Hoofd E, Hommes K, van Sark W. A system perspective to the deployment of flexibility through aggregator companies in the Netherlands. Energy Policy 2018;118:534–51. https://doi.org/10.1016/j.enpol.2018.03.073.
[10] Burger S, Chaves-Ávila JP, Batlle C, Pérez-Arriaga IJ. A review of the value of aggregators in electricity systems. Renew Sust Energy Rev 2017;77:395–405. https://doi.org/10.1016/j.rser.2017.04.014.
[11] Lampropoulos I, Alskaif T, Blom J, van Sark W. A framework for the provision of flexibility services at the transmission and distribution levels through aggregator companies. Sust Energy Grids Networks 2019:100187. https://doi.org/10.1016/j.segan.2018.100187.
[12] van der Stelt S, AlSkaif T, van Sark W. Techno-economic analysis of household and community energy storage for residential prosumers with smart appliances. Appl Energy 2018;209:266–76. https://doi.org/10.1016/j.apenergy.2017.10.096.
[13] Terlouw T, AlSkaif T, Bauer C, van Sark W. Multi-objective optimization of all-electric residential energy systems with heat and electricity storage (submitted and under review). Applied Energy, 2019.
[14] AlSkaif T, Luna AC, Zapata MG, Guerrero JM, Bellalta B. Reputation-based joint scheduling of households appliances and storage in a microgrid with a shared battery. Energy Build 2017;138:228–39. https://doi.org/10.1016/j.enbuild.2016.12.050.
[15] Parra D, Norman SA, Walker GS, Gillott M. Optimum community energy storage system for demand load shifting. Appl Energy 2016;174:130–43. https://doi.org/10.1016/j.apenergy.2016.04.082.
[16] Sardi J, Mithulananthan N, Gallagher M, Hung DQ. Multiple community energy storage planning in distribution networks using a cost-benefit analysis. Appl Energy 2017;190:453–63. https://doi.org/10.1016/j.apenergy.2016.12.144.
[17] Stephan A, Battke B, Beuse MD, Clausdeinken JH, Schmidt TS. Limiting the public cost of stationary battery deployment by combining applications. Nat Energy 2016;1(7). https://doi.org/10.1038/nenergy.2016.79.
[18] Nykamp S, Bosman MG, Molderink A, Hurink JL, Smit GJ. Value of storage in distribution grids-competition or cooperation of stakeholders? IEEE Trans Smart Grid 2013;4(3):1361–70. https://doi.org/10.1109/TSG.2013.2254730.
[19] Ayón X, Moreno MÁ, Usaola J. Aggregators’ optimal bidding strategy in sequential day-ahead and intraday electricity spot markets. Energies 2017;10(4):450. https://doi.org/10.3390/en10040450.
[20] El-Batawy SA, Morsi WG. Optimal design of community battery energy storage systems with prosumers owning electric vehicles. IEEE Trans Ind Inform 2018;14(5):1920–31. https://doi.org/10.1109/TII.2017.2752464.
[21] Soares J, Fotouhi Ghazvini MA, Vale Z, de Moura Oliveira PB. A multi-objective model for the day-ahead energy resource scheduling of a smart grid with high penetration of sensitive loads. Appl Energy 2016;162:1074–88. https://doi.org/10.1016/j.apenergy.2015.10.181.
[22] Arghandeh R, Woyak J, Onen A, Jung J, Broadwater RP. Economic optimal operation of Community Energy Storage systems in competitive energy markets. Appl Energy 2014;135:71–80. https://doi.org/10.1016/j.apenergy.2014.08.066.
[23] Azizivahed A, Naderi E, Narimani H, Fathi M, Narimani MR. A new bi-objective approach to energy management in distribution networks with energy storage systems. IEEE Trans Sust Energy 2018;9(1):56–64. https://doi.org/10.1109/TSTE.2017.2714644.
[24] Nitta N, Wu F, Lee JT, Yushin G. Li-ion battery materials: present and future. Mater Today 2015;18(5):252–64. https://doi.org/10.1016/j.mattod.2014.10.040.

[25] Luo X, Wang J, Dooner M, Clarke J. Overview of current development in electrical energy storage technologies and the application potential in power system operation. Appl Energy 2015;137:511–36.
[26] Li L, Liu P, Li Z, Wang X. A multi-objective optimization approach for selection of energy storage systems. Comput Chem Eng 2018;115:213–25.
[27] Wang X, Palazoglu A, El-Farra NH. Operational optimization and demand response of hybrid renewable energy systems. Appl Energy 2015;143:324–35.
[28] Malhotra A, Battke B, Beuse M, Stephan A, Schmidt T. Use cases for stationary battery technologies: a review of the literature and existing projects. Renew Sust Energy Rev 2016;56:705–21. https://doi.org/10.1016/j.rser.2015.11.085.
[29] Schmidt TS, Beuse M, Xiaojin Z, Steffen B, Schneider SF, Pena-Bello A, et al. Additional emissions and cost from storing electricity in stationary battery systems. Energy Environ Sci 2019. under review.
[30] Sugiyama M. Climate change mitigation and electrification. Energy Policy 2012;44:464–8. https://doi.org/10.1016/j.enpol.2012.01.028.
[31] Cox B. Mobility and the energy transition: a life cycle assessment of swiss passenger transport technologies including developments until 2050. Phd thesis, ETHZ; 2018. < https://www.research-collection.ethz.ch/handle/20.500.11850/276298 > .
[32] Fischer D, Wolf T, Wapler J, Hollinger R, Madani H. Model-based flexibility assessment of a residential heat pump pool. Energy 2017;118:853–64. https://doi.org/10.1016/j.energy.2016.10.111.
[33] Wankmüller F, Thimmapuram PR, Gallagher KG, Botterud A. Impact of battery degradation on energy arbitrage revenue of grid-level energy storage. J Energy Storage 2017;10:56–66. https://doi.org/10.1016/j.est.2016.12.004.
[34] Terlouw T, Zhang X, Bauer C, Alskaif T. Towards the determination of metal criticality in home-based battery systems using a Life Cycle Assessment approach. J Clean Prod 2019. under review.
[35] Xu B, Oudalov A, Ulbig A, Andersson G, Kirschen DS. Modeling of lithium-ion battery degradation for cell life assessment. IEEE Trans Smart Grid 2018;9(2):1131–40. https://doi.org/10.1109/TSG.2016.2578950.
[36] Hamdy M, Hasan A, Siren K. Applying a multi-objective optimization approach for design of low-emission cost-effective dwellings. Build Environ 2011;46(1):109–23. https://doi.org/10.1016/j.buildenv.2010.07.006.
[37] Fesanghary M, Asadi S, Geem ZW. Design of low-emission and energy-efficient residential buildings using a multi-objective optimization algorithm. Build Environ 2012;49(1):245–50. https://doi.org/10.1016/j.buildenv.2011.09.030.
[38] Baldick R. Applied optimization: formulation and algorithms for engineering systems vol. 9780521855. Cambridge University Press; 2006.
[39] Gurobi. Gurobi optimization - the state-of-the-art mathematical programming solver; 2018. < http://www.gurobi.com/ > .
[40] Weber C. Adequate intraday market design to enable the integration of wind energy into the European power systems. Energy Policy 2010;38(7):3155–63. https://doi.org/10.1016/J.ENPOL.2009.07.040.
[41] Carbon Tracker. EU carbon prices could double by 2021 and quadruple by 2030 - carbon tracker initiative; 2018. < https://www.carbontracker.org/eu-carbon-prices-could-double-by-2021-and-quadruple-by-2030/ > .
[42] Swissolar. KEV-EIV-Vergütungssätze gültig für neue Bescheide Quelle: Swissgrid; 2018. < https://www.swissolar.ch/fileadmin/user_upload/Swissolar/Unsere_Dossiers/KEV-Tarife_de.pdf > .
[43] BFE. Wichtigste Neuerungen im Energierecht ab 2018; 2017. < https://www.newsd.admin.ch/newsd/message/attachments/50166.pdf > .
[44] Bauer C, Hirschberg S, Bäuerle Y, Biollaz S, Calbry-Muzyka BC, Heck T, et al. Potentials, costs and environmental assessment of electricity generation technologies. Tech rep. PSI, WSL, ETHZ, EPFL. Paul Scherrer Institut, Villigen PSI, Switzerland; 2017.
[45] Boogen N, Datta S, Filippini M. Demand-side management by electric utilities in Switzerland: analyzing its impact on residential electricity demand. Tech Rep. May, ETHZ; 2016.
[46] Groupe-e. Tarif unique Tarif double/ Doppeltarif ehemals Easy; 2018.
[47] BFS. Bevölkerung verbringt täglich eineinhalb Stunden im Verkehr. Tech rep. BFS; 2017. < https://www.bfs.admin.ch/bfs/de/home/aktuell/neue-veroeffentlichungen.assetdetail.1840420.html > .
[48] Kannan R, Turton H. Long term climate change mitigation goals under the nuclear phase out policy: the Swiss energy system transition. Energy Econ 2016;55:211–22. https://doi.org/10.1016/j.eneco.2016.02.003.
[49] Wernet G, Bauer C, Steubing B, Reinhard J, Moreno-Ruiz E, Weidema B. The ecoinvent database version 3 (part I): overview and methodology. Int J Life Cycle Assess 2016;21(9):1218–30. https://doi.org/10.1007/s11367-016-1087-8.
[50] Ecoinvent. ecoinvent 3.4; 2018. < https://www.ecoinvent.org/database/ecoinvent-34/ecoinvent-34.html > .
[51] IPCC. Fifth Assessment Report - Climate Change 2013. Tech rep. IPCC; 2013.
[52] Swissgrid. Grid data; 2018. < https://www.swissgrid.ch/en/home/operation/grid-data.html > .
[53] Baumann M, Peters DJ, Weil DiM, Grunwald PDA. CO2 footprint and life-cycle costs of electrochemical energy storage for stationary grid applications. Energy Technol 2017;5:1071–83. https://doi.org/10.1002/ente.201600622.
[54] EPEX. Auction — EPEX SPOT; 2018. < https://www.eex.com/en/market-data/power/spot-market/auction > .
[55] Abrell J. The swiss wholesale electricity market. Tech Rep. May, ETHZ; 2017.
[56] Swissgrid. General Balance Group Regulations General regulations relating to the Balance Group Contract; 2015. < https://www.swissgrid.ch/dam/swissgrid/customers/topics/legal-system/balance-group/2/150430-AllgemeineBilanzgruppenRegelungen-V1-8-EN.pdf > .
[57] Weron R. Electricity price forecasting: a review of the state-of-the-art with a look into the future. Int J Forecast 2014;30(4):1030–81. https://doi.org/10.1016/j.ijforecast.2014.08.008.
[58] Zhang Y, Beaudin M, Zareipour H, Wood D. Forecasting Solar Photovoltaic power production at the aggregated system level. 2014 North American power symposium, NAPS 2014 2014. p. 1–6. https://doi.org/10.1109/NAPS.2014.6965389.
[59] Jifri MH, Hassan EE, Miswan NH. Forecasting performance of time series and regression in modeling electricity load demand. 2017 7th IEEE international conference on system engineering and technology (ICSET) IEEE; 2017. p. 12–6. https://doi.org/10.1109/ICSEngT.2017.8123412.
[60] Vaghefi A, Jafari M, Bisse E, Lu Y, Brouwer J. Modeling and forecasting of cooling and electricity load demand. Appl Energy 2014;136:186–96. https://doi.org/10.1016/j.apenergy.2014.09.004.
[61] Pappas SS, Ekonomou L, Karamousantas DC, Chatzarakis GE, Katsikas SK, Liatsis P. Electricity demand loads modeling using Auto Regressive Moving Average (ARMA) models. Energy 2008;33(9):1353–60. https://doi.org/10.1016/j.energy.2008.05.008.
[62] Akaike H. A new look at statistical model identification. IEEE Trans Autom Control 1974;19(6):716–23. https://doi.org/10.1109/TAC.1974.1100705.
[63] Hyndman RJ, Kostenko AV, et al. Minimum sample size requirements for seasonal forecasting models. Foresight 2007;6(Spring):12–5.
[64] Antonanzas J, Osorio N, Escobar R, Urraca R, Martinez-de Pison FJ, Antonanzas-Torres F. Review of photovoltaic power forecasting. Solar Energy 2016;136:78–111. https://doi.org/10.1016/j.solener.2016.06.069.
[65] Hewicker Christian Werner Oliver RJ, Michael Ebert, Tim Mennel, Nynke Verhaegh. Energiespeicher in der Schweiz Bedarf, Wirtschaftlichkeit und Rahmenbedingungen im Kontext der Energiestrategie 2050. Tech Rep. BFE, BFE; 2013.
[66] Branke J, Deb K, Miettinen K, Slowinski R. Multiobjective optimization: interactive and evolutionary approaches vol. 5252. Springer; 2008. https://doi.org/10.1007/978-3-540-88908-3.
[67] Naderi E, Azizivahed A, Narimani H, Fathi M, Narimani MR. A comprehensive study of practical economic dispatch problems by a new hybrid evolutionary algorithm. Appl Soft Comput 2017;61:1186–206.
[68] Lokeshgupta B, Sivasubramani S. Multi-objective dynamic economic and emission dispatch with demand side management. Int J Electr Power Energy Syst 2018;97:334–43.
[69] Narimani H, Razavi S-E, Azizivahed A, Naderi E, Fathi M, Ataei MH, et al. A multi-objective framework for multi-area economic emission dispatch. Energy 2018;154:126–42.
[70] Sou KC, Kordel M, Wu J, Sandberg H, Johansson KH. Energy and co 2 efficient scheduling of smart home appliances. 2013 European control conference (ECC). IEEE; 2013. p. 4051–8.
[71] Azizivahed A, Narimani H, Fathi M, Naderi E, Safarpour HR, Narimani MR. Multi-objective dynamic distribution feeder reconfiguration in automated distribution systems. Energy 2018;147:896–914.
[72] Deb K. Multi-objective optimization. Search methodologies. Springer; 2014. p. 403–49.
[73] Cheng C-C, Lee D. Return on investment of building energy management system: a review. Int J Energy Res 2018:1–20. https://doi.org/10.1002/er.4159.
[74] AlSkaif T, Lampropoulos I, van den Broek M, van Sark W. Gamification-based framework for engagement of residential customers in energy applications. Energy Res Soc Sci 2018;44:187–95. https://doi.org/10.1016/j.erss.2018.04.043.